University of Alberta

A Method to Enhance Re-Endothelialization of Tissue Engineered
Decellularized Allograft Heart Scaffolds

by

Leena Sunil Desai

A thesis submitted to the Faculty of Graduate Studies and Research
in partial fulfillment of the requirements for the degree of

Master of Science

Experimental Surgery

Department of Surgery

©Leena Sunil Desai
Fall 2009
Edmonton, Alberta

Examining Committee

Dr. Gregory Korbutt, Surgery

Dr. Steven Meyer, Surgery

Dr. David Ross, Surgery

Dr. Bernard Thébaud, Pediatrics

ABSTRACT

Allograft tissue is used to reconstruct cardiac birth defects but induces an immune response resulting in allo-sensitization. Decellularization reduces the immune response, however, acellular vascular tissue is thrombogenic. *In-vitro* endothelialization may attenuate thrombogenicity. Here we offer our work, which determines a novel method of endothelial cell attachment using Arginine-Glycine-Aspartic Acid (RGD) peptides.

We show that an RGD-FITC peptide can be bound to a decellularized ovine cardiac scaffold. RGD modification increases HUVEC cell adhesion to the surface at 3 days of static incubation *in-vitro* compared to decellularized tissue alone. Repetition using a decellularized human scaffold shows similar results. Cleavage of the potentially immunogenic FITC label retains our RGD peptide.

In summary, we determine that decellularized allografts show enhanced HUVEC cell adhesion when modified with an RGD peptide under static conditions. This may increase cell retention *in-vivo* leading to a decellularized cardiac allograft repopulated with functional autologous cells from the recipient.

ACKNOWLEDGEMENTS

I would like to thank the Graduate students of the ADI and the Department of Surgery for their camaraderie and humor. It was a pleasure working amongst you.

Lastly I wish to express immeasurable gratitude to my friends and family, who offered support, laughter, and constant motivation. I would like to particularly thank my parents who have stood by my side tirelessly throughout the duration of this work.

TABLE OF CONTENTS

LIST OF TABLES

LIST OF FIGURES

FIGURE   **DESCRIPTION**
          PAGE

LIST OF ABBREVIATIONS

AA	Amino acid
AV	Atrioventricular
BMSC	Bone Marrow Stem Cells
CMRL	Connaugh Medical Research Laboratory Cell Culture Medium
DAPI	4',6-diamidino-2-phenylindole
DMSO	Dimethyl Sulfoxide
DNAse	Deoxyribonuclease
DTT	Dithiothreitol
EC	Endothelial Cell
ECM	Extracellular Matrix
EDC	1-Ethyl-3-[3-dimethylaminopropyl]carbodiimide hydrochloride
EDTA	Ethylenediaminetetraacetic Acid
EMCH	[N-e-Maleimidocaproic acid] hydrazide
eNOS	Endothelial Nitric Oxide Synthase
ePTFE	Expanded Polytetrafluoroethylene
FACS	Fluorescent Activated Cell Sorting
FBS	Fetal Bovine Serum
FITC	Fluorescein isothiocyanate
FN	Fibronectin
GAG	Glycosaminoglycans
H&E	Hematoxylin & Eosin
HEPES-BSS	HEPES Buffered Saline Solution
HLA	Human Leukocyte Antigen
HLHS	Hypoplastic Left Heart Syndrome
HPLC	High Performance Liquid Chromatography
HUVEC	Human Umbilical Vein derived Endothelial Cell
IVIG	Intravenous Immunoglobulin
KCl	Potassium Chloride
MES	2-[morpholino]ethanesulfonic acid
MMP	Matrix Metalloproteinase
MSC	Mesenchymal Stem Cells
NGS	Normal Goat Serum
PBS	Phosphate Buffered Saline
PHSRN	Proline-histidine-serine-arginine-asparagine
PMSF	Phenylmethanesulphonylfluoride
PRA	Panel Reacive Antibodies
RFU	Relative Fluorescence Units
RGD	Arginine-glycine-aspartic acid
RNAse	Ribonuclease
RVPA	Right Ventricular Pulmonary Artery
Sulfo-NHS	N-hydroxysulfosuccinimide
TFA	Trifluoroacetic Acid
TIMP	Matrix Metalloproteinase Inhibitor
TNS	Trypsin Neutralizing Serum

UCB	Umbilical Cord Blood
UPW	Ultrapure Water
UV	Ultraviolet
VEC	Valvular Endothelial Cell
VEGFR2	Vascular Endothelial Growth Factor Receptor 2
VIC	Valvular Interstitial Cell
VWF	Von Willebrand Factor

1   GENERAL INTRODUCTION

Advancements in congenital cardiac surgery have improved the lives of children suffering from congenital cardiac disease significantly. However, major challenges still remain to be resolved regarding surgical replacement of heart valves. Currently, the limited availability of human (allograft) cardiac donor tissue for use in surgical repair of malformations is a concern. While little can be done to assuage this scarcity in tissue, surgical research can focus upon creating an alternative to the current tissues that may ease this burden. Congenital surgery very often utilizes a heart valve or conduit for repair of birth defects such as hypoplastic left heart syndrome (HLHS). An ideal heart valve to replace existing alternatives for surgical repair would illicit a minimal immune reaction, maintain durability, resist infection, be non-thrombogenic and, most importantly in the pediatric population, have the ability to grow in proportion to the child (1).

Despite the advancements made in congenital surgery, an ideal heart valve replacement still does not exist. In its place are synthetic materials such as Dacron® conduits and mechanical heart valves or xenogeneic tissues such as porcine valves. Neither mechanical nor xenogeneic valves are ideal, however. Both increase chances of infection (2) through fungal and bacterial inoculation and illicit increased inflammatory responses in the recipient. Mechanical valves require anticoagulation with Coumadin (3) and xenogeneic valves have limited durability (4) and calcify quickly. Allograft (i.e. human) heart valves and vessels are commonly used in surgical repair due to their superior handling capabilities

and excellent hemodynamics (5). Potential complications of allograft tissue include damage after cryopreservation, size mismatch and infection (6). In addition, researchers and clinicians alike are recognizing a detrimental humoral and cell-mediated immune response that devastates the valve, *in-vivo* (7,8). The cell-mediated attack of foreign antigens present on the allograft possibly leads to valve destruction and degeneration (9). This leads to an increased need for reoperation, which in turn results in an increased risk of mortality and morbidity (10). To compound matters, increased reoperation may have lasting negative physiological (11) and cardiac transplantation may have neuropsychological effects on children, through immunosuppression and rejection (12). The humoral immune response, however, causes more lasting negative effects by sensitizing the patient to the foreign tissue and generating anti-HLA antibodies in the host (13). These antibodies can then complicate future transplants, should reoperation be necessary.

There are two options to minimize the immune response to implanted allografts: 1) alter the host, usually via immunosuppression; or 2) alter the valve. Immunosuppression has been shown to have many side effects including lasting fine motor complications in the cognitive development of children. Decellularization of the allograft valve attenuates both the humoral and the cellular immune response *in-vitro* and *in-vivo* (14). However, although decellularized valves possess favorable immunogenic characteristics, these valves are highly thrombogenic (15). Indeed, decellularized grafts have thrombosed *in-vivo* (14). The increased risk of thrombosis in these valves is attributed to the

removal of the valvular endothelial cell lining in the decellularization process. *In-vitro* endothelialization of the decellularized vascular tissue prior to implantation attenuates its thrombogenicity (16,17).

The current research initiative is to find an effective method to re-endothelialize the surface of decellularized tissue. Potentially, if a source of CD34+ stem cells were available these could be utilized to repopulate the acellular tissue. Human umbilical cord blood (UCB) is rich in CD34+ stem cells and banking is performed with increasing frequency facilitating easy translation to the clinical setting. Umbilical cord blood stem cells (UCBSC) have the capacity to form a greater number of colonies and a higher cell cycle rate thereby shortening the preparation time (18). Compared with other stem cell sources, the advantageous characteristics of UCBSC are their availability, shortened time to transplantation, lower risk of transmission of viral infectious diseases, reduced immunological reactivity, potentially lower risk of immunological rejection, and lower risk and severity of acute and chronic graft versus host diseases. While the potential for UCBSC for heart valve lining has been explored, the methods previously documented are lengthy and expensive, making them impractical for clinical translation. Instead, a novel method of attachment using RGD ligand peptides may decrease the preparation time and cost for these valves, resulting in decreased time to transplant (19). By using the patients' own endothelial cells derived from their own umbilical cord blood to repopulate a decellularized valve, a custom heart valve could potentially be available at the time of birth. In addition, this valve may even have the potential to grow, leading to a non-

immunogenic custom heart valve replacement that could endure for the patients'

entire life and eliminate the need for re-transplantation later in life.

1.1 NATIVE VALVE FUNCTION

Normal blood flow through the heart is vital for body function and health.

The heart valves are integral to proper heart function. The normal heart contains

four valves: two atrioventricular and two semilunar. The atrioventricular valves

(right tricuspid and left mitral) ensure positive blood flow from the atria to the

ventricles. The semilunar valves (pulmonary and aortic) maintain blood flow from

the ventricles to the lungs and aorta, respectively. Normal heart valves do not

allow backward flow of blood (regurgitation) during systolic or forward flow, nor

do they exhibit a pressure gradient at this time (20). Thus, cardiac output is a key

measurement of cardiac function (21). With respect to heart valves, cardiac output

efficiency may be defined through the effectiveness of coupling of the heart to the

artery as measured by the coupling ratio (Ea/Ees) with optimal values between 0.6

to 1.2 (22).

Mitral valves are attached to the ventricular wall by chordae tendonae,

which are in turn attached to papillary muscles that mediate the opening and

closing of the valves according to the pressure across the valve. The mitral valve

plays an important role in maintaining the heart structure by anchoring the fibrous

skeleton of the heart and the extracellular matrix through the chordae tendinae and

the papillary muscles (23). This is supported by the loss of shape and function of

the heart upon removal of the chordae tendinae (24). If these structures are

removed, the ventricle is no longer able to maintain its shape, leading to

dysfunctional contraction, dilation and afterload increase (25) thereby lowering

the efficiency of cardiac output mentioned earlier.

Arterial valves work in a similar fashion but utilize pressure gradients to

open and close as opposed to muscular mediation. Ventricular contraction raises

the pressure in the ventricle, causing the valve to open. This allows blood to flow

freely out of the heart and into the artery without resistance (20). The outward

flow of blood lowers the pressure in the ventricle, which then forces the valve to

close and prevent backflow.

1.1.1   NATIVE VALVE COMPONENTS

There are several key characteristics required by healthy valves to

maintain forward blood flow including durability, viability, injury mediated repair

remodeling and mechanical stress strength (26). These characteristics are

dependent upon the integrity of specific structures and components of the valve.

The important structures of the semilunar valves are the cusps and the aortic and

pulmonary roots, while the important AV valve components are the leaflets,

chordae tendineae, papillary muscles and myocardium. The importance of these

structures in valve function has already been outlined.

1.1.1.1   EXTRACELLULAR MATRIX

The valvular extracellular matrix (ECM) is primarily responsible

for maintaining valve durability. Microscopically, there are three distinct layers

which make up the ECM: 1) the ventricularis 2) fibrosa and 3) spongiosa. The

ventricularis is made up mostly of elastin, while the fibrosa is mostly collagen.

The spongiosa is comprised of mostly glycosoaminoglycans (GAGs) (Figure 1-1)(26).

In addition to the ECM, the valve is populated with two specific cell types: 1) endothelial cells and 2) interstitial cells. Endothelial cells line the surface of the valve that comes into contact with blood while interstitial cells are located primarily in the interior of the valve (see Figure 1-1). These cells in particular play extremely important roles in the function of healthy native valves.

1.1.1.2 INTERSTITIAL CELLS

Valvular interstitial cells (VICs) are the most numerous cell type in the valve (26). They are primarily responsible for synthesizing the ECM. They express many molecules including matrix degrading enzymes, metalloproteinase's (MMPs) and MMP inhibitors (TIMPs), which are all responsible for matrix remodeling (27). In normal valves VICs exhibit a phenotype similar to fibroblasts. Myofibroblasts, specifically, are activated fibroblasts that are responsible for tissue remodeling and wound healing through synthesis of the ECM (28). Studies have shown that when VIC distribution is impaired, the ECM integrity is degraded as seen by leaflet thickening and disorganization of collagen and GAGs (29). These cells, then, are vital for maintaining valve durability and structure.

1.1.1.3 ENDOTHELIAL CELLS

In general, endothelial cells are responsible for regulating immune and inflammatory responses as well as facilitating non-thrombogenic blood-tissue interfaces. Valvular endothelial cells (VECs) however, differ from those found in normal circulation (30). VEC alignment along the surface of the valve is

perpendicular in response to the shear stress in the artery (31). This perpendicular alignment allows for unidirectional blood flow (30). In addition, studies have shown that VECs regulate VIC phenotype and therefore ECM regenesis (32). VEC dysfunction has been shown to have detrimental effects to the valve including increased thrombosis and cardiovascular risk (33, 18).

1.2 CARDIAC SURGERY

1.2.1 CONGENITAL CARDIAC SURGERY

While the outcome of many surgical techniques have improved drastically in the recent past, the quest for perfection, in this field at least, has led to an entire section of scientific medical research dedicated to congenital valvular surgery. With a worldwide incidence of 0.6%, congenital heart disease is a substantial health concern (34). When evaluating the number of children with congenital heart disease requiring surgical treatment, the number increases to include 0.3 to 1% of cases, in western countries (35). Generally, congenital cardiac disease encompasses many fields including cardiology, palliative care, pharmacology and surgery. Congenital heart surgery benefits from advancements in all these fields, and recently there has been an increased trend in surgical repair versus palliative care (10), due mostly to improved survival after surgery. Those patients undergoing surgical repair for congenital defects often require reconstruction of major blood vessels, and often require valve replacements. As a result, there is an increasing need for an ideal valve prosthesis.

1.2.2 VALVULAR SURGERY

Degenerative valve disease has become the most prevalent presentation of valvular heart disease in first world countries (36) with aortic valve disease being the third most common cause of heart disease. Each year in the United States, approximately 95 000 valve procedures are performed (37). Calculating the economic value and impact of these procedures is now an increasingly studied area of interest. In 4617 patients operated on between 1961 and 2003 the cost-effectiveness was $13 528 per quality-adjusted life year gained after surgery, with $27 182 specifically in the younger age bracket (38). Diseased cardiac valves often require reconstruction or in some cases, replacement, especially in young children with congenital heart defects.

Human allograft valves were first utilized for replacement of diseased valves in 1962 (39) and for reconstruction in 1966 (40). Surgical techniques include the Ross, Yacoub and David procedures. The Ross procedure entails the transposition of the patients' own pulmonary valve to the aortic position in the same patient (autograft) and replacement of the pulmonary valve with an alternative valve; often an allograft pulmonary valve (41,42). However, this surgery has also been associated with high early mortality in very young patients (43). The Yacoub method is a remodeling technique and the David procedure involves the resuspension of a prosthetic valve within the implanted graft. Neither technique, however, is perfect as both result in increased valve leaflet stress (44). Valve replacements remain the more commonly performed surgical intervention. Thus, while surgical technique has improved drastically over the years, the lack of an appropriate valve replacement has impeded complete success in this field.

1.2.3 VALVULAR SURGERY: SUCCESS WITH LIMITATIONS

Though the number of successful pediatric cardiac surgeries continues to rise, more and more researchers and clinicians are noting increasing valve and graft failure. Ultimately, many allografts will fail with a freedom from reoperation for all causes of 69% at 15 years (45). In younger children (age 3 and under) the failure rate is higher, with a reoperation rate of 60% and 1.9 years mean interval for replacement after their first operation (46). Procedures such as Ross are likewise controversial since the procedure only serves a small patient population and many of these patients will require reoperation later in life (47). The actual act of surgical intervention alone contributes to increased neuropsychological damage including lowered fine motor skills in children (34) although recently, a switch to RVPA surgical repair of HLHS resulted in improved psychomotor outcomes after 2 years (48). Importantly, the success of surgical interventions varies greatly from institution to institution indicating a plethora of variables that are responsible for surgical outcomes in the pediatric population. A heart valve that has the potential to grow and repair itself in concordance with the child may assuage the discrepancies in the surgical field and the reliance on surgical experience, to help standardize the anomalies between institutions. Presently, there are three types of valves used in congenital cardiac surgery for valve replacement and reconstruction: 1) allografts 2) xenografts and 3) mechanical.

1.2.4 ALTERNATIVE VALVE OPTIONS:

Xenografts would present an ideal valve replacement due to availability, however, they are problematic when implanted. These valves tend to deteriorate with time at an increased rate in children (49,50). In addition, they are at

increased risk of infection and thrombosis. The long-term durability of xenograft stentless valves significantly decreases after 8 years (51), which is especially problematic in young children for whom reoperation is detrimental.

Mechanical valves are likewise an option due to availability. These valves tend to have a much higher incidence of thrombosis, however, which makes them unsuitable as an ideal replacement. Patients with mechanical heart valves require life-long anticoagulation therapy. With children this puts them at increased risk for bleeding related adverse effects (35,52).

Allografts have an advantage over the others as they have superior hemodynamics, resistance to infection, excellent durability and freedom from anticoagulation and thrombosis (53). Compared to xenografts, allografts have a lower incidence of valvular obstructions once implanted (54). However, allografts tend to show high levels of degeneration *in-vivo*. Especially at a younger age there is an increased risk of degeneration (55). Degeneration does not only occur as a result of *in-vivo* conditions. Studies have indicated that cryopreservation methods of allograft valves can lead to decreased structural integrity of the valve as well. There is increased cusp tissue degeneration (56). It would seem that the cryopreservation method itself leads to increased likelihood of valve destruction and injury (57) likely due to the preservation of allogeneic cell components. There is a reduction in the amount of calcification between ice-free and iced cryopreservation methods (58), however, the calcification was still significant for both methods. This creates challenges surrounding methods for allograft storage and preservation between donor time and recipient surgery.

Increasingly, researchers have begun to study the effects of the recipient immune system on the donor graft. It has been shown that HLA mismatch to the foreign donor tissue has led to aortic valve deterioration (59). A specific cell mediated response to the foreign graft is fast and effective, resulting in leaflet infiltration after a week, and total leaflet destruction within 4 weeks (60). In addition to this vigorous cell mediated response, there has been increasing concern over activated B-cell mediated humoral immunity in children. This humoral response, measured primarily as panel reactive antibodies (PRA) shows increased PRA levels which peak at 6 months after transplant (61). These PRA levels may lead to more rapid failure of a second allograft, if and when reoperation becomes necessary (62).

1.3   TISSUE ENGINEERING:

Despite the detrimental effects of the recipient immune response to transplanted valves, allograft tissue seems to be the best available option for surgical repair. Due to its superior hemodynamics and durability, a possible mechanism to improve an engineered valve would be to alleviate the immune response to these allografts. It was thought that intravenous immunoglobulin therapy (IVIG) treatment would attenuate host sensitization; however, prophylactic treatment of the patient with IVIG does not prevent recipient sensitization to the implanted valve in neonates (63). Thus, an alternative to modifying the patient is necessary to attenuate the valve-induced immune response.

1.3.1 DECELLULARIZATION

Decellularization is a highly effective technique used to modify the valve in order to eliminate the immune response. While a variety of methods for decellularization have been tested (64-66) 48hr incubation with a series of hypertonic and hypotonic Tris buffers containing Triton-X-100 followed by a 72hr washout in phosphate-buffered saline solution has the most effective cellularity reduction while maintaining matrix integrity (67). Comparison of this technique to an enzymatic decellularization with trypsin/EDTA, which was likewise found to completely decellularize the graft, resulted in destruction of the valve ECM in the same study (67). Thus, detergent-based decellularized methods seem to be the most effective at removing cellular elements that stimulate the immune response while preserving structural integrity. Importantly, complete decellularization is necessary in order to attenuate the immune and inflammatory response as was seen in the case of the Synergraft decellularized porcine valve implanted in pediatric children in Europe. Incomplete decellularization led to rapid degradation, structural failure and devastating results (68). In addition, the xenogenic antigens may have played a role in the early failure of these grafts *in-vivo*; this will be discussed in more detail later in this chapter. If complete decellularization is achieved and these grafts are implanted *in-vivo*, decellularization eliminates both the cell-mediated and the humoral immune response in rats (14) and has been shown to drastically reduce the calcification of homografts transplanted into a sheep model (69) with preserved durability and functionality. The integrity of the ECM allows for repeated loading and unloading during the cardiac cycle and thus the preservation of the biomechanical properties

of decellularized tissues is paramount to their clinical applicability. It has been

shown that osmotic decellularization, similar to the method used in our

investigations maintains tissue ECM integrity with comparable stress at fracture

values and elastic modulus as well as echocardiographic data (70). Interestingly,

cryopreservation may influence the viability of these tissues. In a study comparing

the effects of cryopreservation on decellularized tissue durability showed that

after freezing there were no major changes in biomechanical properties of the

tissues, however, increased strain after stress was noted after cryopreservation

(71). Decellularization has been shown to decrease the collagen crimp of ECM

(72), which may influence the long-term durability of these tissues. However the

use of these decellularized tissues *in-vivo* has not shown any structural failure

after 12 months (69) which is promising. Decellularization of tissues thus

provides a viable and efficacious scaffold for tissue engineering studies.

1.3.2   DECELLULARIZATION: Success with Limitations
Unfortunately, decellularization alone is not enough to create the ideal

valve replacement. While these valves have preserved functionality and do not

illicit a response from the recipients' immune response, they are much more prone

to thrombosis *in-vivo* (73). This is due, most likely, to the loss of endothelial cells.

Endothelial cells are responsible for preventing contact between circulating

platelets and the collagen surface of vascular tissues (74). Activated platelet

adhesion is seen with decellularized tissue, however this platelet activation is

attenuated after cell seeding (75). In addition to platelet adhesion, decellularized

tissue also showed an increased migration of inflammatory cells despite

completeness of the decellularization process (76). This increased inflammatory response may be abrogated by recellularization. Many researchers now aim to modify existing heart valves or prosthetic scaffolds with endothelial cells in order to create a living, functional valve that is not thrombogenic.

1.3.3 RECELLULARIZATION

Efforts to create or modify existing heart valves have led to many recent advances in the field of cardiac tissue engineering. The importance of the endothelial cell layer has been identified through work in the field of decellularization. Researchers aim to repopulate numerous scaffolds, both biological and prosthetic with endothelial cells. It has been shown that decellularized (16) and prosthetic (77) valves alike will not re-endothelialize *in-vivo* after 4 weeks. In addition, prosthetic expanded polytetrafluoroethylene (ePTFE) will not endothelialize with endothelial cells alone. Freeze-dried porcine pulmonary valves have been repopulated with vascular endothelial cells and fibroblasts to confluency (78), however, this will not reduce the immune response to the xenogeneic graft without further modification. Recellularization in the systemic circulation is also seen in decellularized xenografts in large animal model of dogs (79). This may be promising as xenografts can be shown to not induce an inflammatory response. *In-vivo* studies have shown that repopulation of acellular porcine valves with circulating endothelial cells is possible after 24 weeks with minimal calcification (80). The luminal surface of decellularized tissue stains positive for fibronectin, and facilitates the migration of CD34+ cells with minimal inflammatory cell staining (81) indicating the biocompatibility of

decellularized grafts. Cryopreservation methods typically involve the use of dimethyl sulfoxide, which can influence both cell viability and recellularization, making it an important aspect of decellularized tissues to study. It has been shown, however, that after thawing, decellularized tissues do not retain residual DMSO (82) indicating the ability of these tissues to be used for tissue engineering purposes without concern of cellular compromise upon re-cellularization. In addition, nanoscale topography analysis of the basement membrane of decellularized tissue shows adequate pores and elevations to support recellularization (83). The recellularization of decellularized tissues will likely need to include both endothelial cells, to prevent thrombosis and also interstitial cells to facilitate collagen synthesis, remodeling and growth. Thus, suitable methods for re-endothelialization and re-interstitialization will need to be examined.

1.3.3.1   RE-INTERSTITIALIZATION

Mesenchymal stem cells (MSCs) have been shown to exhibit many of the cell surface markers present in valvular interstitial cells (84). Thus, MSCs have great potential for use in re-interstitialization of decellularized tissues. One method for re-interstitialization would be to adhere MSCs to the surface of decellularized grafts in the hopes that under physiological conditions, either simulated or real, these MSCs will migrate into the ECM and embed themselves therein to regain normal VIC function. MSC enhanced binding to decel tissues has been shown using anti CD-90 antibodies adsorbed onto the luminal surface, however, MSC migration into the ECM was not seen (85). MSC cells injected

directly into the ECM showed decreased inflammation *in-vivo* compared to bone marrow derived stem cells (BMSCs) indicating that MSCs are the best source for re-interstitialization and that repopulation of the ECM is possible using a direct method of cell addition (86), rather than cellular migration. Interestingly, these transplanted tissues showed slight re-endothelialization *in-vivo*, upon explant.

1.3.3.2   RE-ENDOTHELIALIZATION

Re-endothelialization of decellularized scaffolds shows promise for attenuating the thrombogenicity of these tissues *in-vivo*. Many groups have successfully re-endothelialized biological scaffolds such as acellular matrices, all with improved results. Re-endothelialization can progress in either an *in-vitro* system, or by implanting tissues and hoping for endothelial cell migration *in-vivo*. *In-vitro* seeding of endothelial cells preclinically showed increased endothelialization compared to decellularized tissues alone after 3 months (87). Pre-seeding using a two step process involving vascular fibroblasts improved endothelial cell function and proliferation compared to adhesion on the luminal surface of decellularized tissue (88). Endothelium attached directly to this tissue still illicited an inflammatory response (89). Pre-seeding *in-vitro* usually involves the use of a bioreactor to facilitate a monolayer of endothelium prior to implantation (90); this will be discussed later in this chapter.

One limitation with tissue engineering of heart valves with endothelial cells, however, does not seem to necessarily be the repopulation; there is a plethora of evidence to show successful re-endothelialization of decellularized cardiac tissue *in-vitro*. The main problem is the lack of endothelial migration in

the peripheral system (91). This complicates the ability to form and maintain a

confluent endothelial monolayer *in-vivo*. It has been shown that pre-seeding of

decellularized tissues prior to implantation shows increased migration of

endothelial progenitor cells to the tissue site *in-vivo* (87). Thus, a source of

endothelial cells is necessary to facilitate fast and easy translation to the clinical

setting. Endothelial progenitor cells derived from umbilical cord blood have 100

times the population doubling capacity of peripheral endothelial cells and can also

continue into higher passages in tissue culture (92). Cryopreserved umbilical cord

blood endothelial cells (UCBECs) seeded onto a prosthetic porous matrix and

seeded in a pulse duplicator have shown excellent growth potential (93).

However, UCBECs can also be seeded *in-vitro* under static conditions to get a

confluent monolayer on decellularized tissue (94) making them very easy to work

with. In addition to decellularized and prosthetic scaffolds, biodegradeable

scaffolds have likewise been successfully seeded in a bioreactor with UCBEC

progenitors (95). Umbilical cord blood derived endothelial cells are a much more

efficient and practical source for endothelial cells used for tissue repopulation.

1.3.3.2.1 FIBRONECTIN
 The extracellular matrix provides a framework for cell adhesion, supports

cell movement, and serves to compartmentalize tissues into functional units (96).

Cell adhesion is mediated by the specific interactions of cell surface receptors

with extracellular glycoproteins. The best characterized integrin ligand is

fibronectin. A disulfide bonded dimer of approximately 230-270kDA subunits

(97), fibronectin is a core component of many extracellular matrices where it

regulates a variety of cell activities through direct interactions with cell surface

integrin receptors (Hynes 1990). The best characterized cell adhesion receptors

are the integrins. Integrins comprise a family of more than 23 noncovalent,

heterodimeric complexes consisting of an alpha and a beta subunit (97). Each

subunit is a glycoprotein with a large, globular extracellular domain and a

transmembrane domain (97). Most integrins have relatively small cytoplasmic

domains consisting of fewer than 60 amino acids. Although many integrins can

bind fibronectin, the $\alpha5\beta1$, integrin is the major fibronectin receptor on most

cells. This integrin mediates such cellular responses to fibronectin substrates as

adhesion, migration, assembly of extracellular matrix, and signal transduction.

Integrin ligands, such as fibronectin, are not passive adhesive molecules but are

active participants in the cell adhesive process that leads to signal transduction.

Fibronectin is a multifunctional glycoprotein comprised of three different types of

homologous repeating units (termed type I, type II, and type III) (99). Fibronectin

has at least two independent cell adhesive regions: one located near the center of

the polypeptide chain in the ninth and tenth type III modules binds to the $\alpha5\beta1$

integrin. The biological function of the central cell adhesive region requires two

critical amino acid sequences--an Arg-Gly-Asp (RGD) sequence and a Pro-His-

Ser-Arg-Asn (PHSRN) sequence, which function in synergy--for optimal binding

to the $\alpha5\beta1$ integrin (100). Furthermore, the spacing between the crucial RGD

and PHSRN sequences is also important for activity, suggesting the sequences

themselves are necessary, but not sufficient, to account for the cell adhesive

activity of fibronectin. (101). The ability of fibronectin to bind cells can be

accounted for by the tetrapeptide L-arginyl-glycyl-L-aspartyl-L-serine, a sequence which is part of the cell attachment domain of fibronectin and present in at least five other proteins. This tetrapeptide may constitute a cellular recognition determinant common to several proteins. (102). Fibronectin is synthesized by many adherent cells including endothelial cells (98), which then assemble it into a fibrillar network. The assembly process is integrin-dependent and fibronectin-integrin interactions initiate a step-wise process involving conformational activation of fibronectin outside and organization of the actin cytoskeleton inside (97). FN binds to transmembrane integrin receptors on adherent cells primarily via the $\alpha5\beta1$ integrin receptor to mediate fibrin assembly (103) (See Figure 2). Integrins link FN to actin cytoskeleton through interactions between cytoplasmic domains and cytoskeletal associated proteins (104). Extracellularly, FN-FN association and fibril formation is promoted by inducing conformational changes in the bound FN (105). During assembly, fibronectin undergoes conformational changes that expose fibronectin-binding sites and promote intermolecular interactions needed for fibril formation (97). Fibronectin and integrins play crucial roles in a variety of morphogenetic processes, in which they mediate cell adhesion, migration, and signal transduction. They induce hierarchical transmembrane organization of cytoskeletal and signaling molecules into multimolecular complexes of more than 30 proteins. Organization of these complexes is a synergistic process dependent on integrin aggregation and occupancy, as well as tyrosine phosphorylation. Integrins also cooperate with growth-factor receptors to enhance signaling. Fibronectin and integrins induce a

variety of downstream effects, including enhanced transcription factor activity, induction of over 30 genes (> half novel), and altered expression of over 100 proteins. Fibronectin and integrins therefore trigger a hierarchy of signaling responses involved in regulating processes crucial for normal morphogenesis, including cell adhesion, migration, and specific gene expression. (106). Fibronectin is known to stimulate cell growth and migration, but research does not provide a complete picture of all the mechanisms involved (107). Clinical studies of coating decellularized tissues with fibronectin prior to *in-vitro* seeding with endothelial cells has shown improved clinical outcomes for the Ross procedure (108). However, decel tissue coated with fibronectin *in-vitro* may not function the same way as native fibronectin. It is likely that the assembly of fibronectin is a highly sensitive process, dependent upon cellular components (109). The decellularization process likely alters native and added fibronectin, changing its ability to expose its binding sites to promote cell adhesion (110). Further studies are needed before practitioners can apply *in-vitro* results to *in-vivo* environments.

1.3.3.2.2 RGD INTEGRIN LIGANDS

It seems evident from recellularization studies that while *in-vitro* recellularization is possible and has been correlated to improved outcomes in living models, the retention of the neo-endothelium and its subsequent ability to hone endothelial progenitor cells for confluent adhesion is limited; this is necessary to promote native EC function. Thus, a method is required for enhancing the efficiency of endothelial cell binding to decellularized allografts.

Pre-coating with FN has been shown to have improved cell retention *in-vivo*, however, for long term functionality of the ECM and the ability to repair and remodel it is likely that *in-vitro* coated FN may not interact with the adherent cells in the same manner as native FN (111). Thus, it may be more beneficial to pre-coat the tissues with the peptide responsible for the initiation of FN secretion and assembly (112). The RGD sequence of FN is well characterized and required in the initiation steps of matrix assembly (112). The RGD sequence in FN is a 10 AA long chain (See Figure 1-2) of which the RGD sequence binds the $\alpha5\beta1$ integrin on adherent cells. RGD peptides are known to be important in facilitating endothelial cell binding. (45,113) via cell surface integrin receptors (46). Integrins bind to RGD peptides and the strength of the interaction (114) is dependent upon residues adjacent to the RGD. A large number of RGD peptides that effectively bind endothelial cells have been described: RGDS (115), GRGDVY (116), GRGDSP (117), G-Pen-GRGDSPCA (cyclic, pen: penicillamine) (117), YAVTGRGDS (118), CGGNGEPRGDTYRAY (119). Numerous variables determine the efficiency of endothelial cell binding (120). Ligand density is known to be important in determining endothelial cell adhesion (121). Determination of allograft ligand density can be performed according to the method through bonding of RGD-FITC to the valve to facilitate measurement. The FITC fragment of the RGD-FITC peptide is liberated from the valve by chymotrypsin digestion and measured by high performance liquid chromatography (HPLC) (19). Endothelial cells can then be seeded onto these valves as described above. The endothelial cell retention on valves bound with

21

RGD peptide is significantly higher than on valves without RGD(39). In all instances, endothelial cells are sloughed off through shear stress if seeded without peptide (122).

To date, no study has shown the binding capacity of RGD peptides onto decellularized tissue. Methods have been published which could be extrapolated to decellularized allografts by exploiting the free carboxyl terminus on the collagen of the ECM and reacting through enzymatic addition of a highly reactive ester group (114). Whether this will enhance endothelial cell binding remains to be seen.

1.3.4 BIOREACTORS

Due to the time taken to repopulate *in-vivo* and the lack of confluency of the endothelial layer formed many researchers are now attempting to repopulate the endothelial monolayer of valves *in-vitro* rather than *in-vivo*. The use of a pulse duplicator or bioreactor to simulate physiological conditions has revolutionized the field of tissue engineering. Indeed, repopulation of endothelial cells *in-vitro* under a bioreactor leads to improved confluence of the monolayer *in-vivo* (123). In addition, interstitial cell migration occurs *in-vivo* as a result of this *in-vitro* seeding (87). Therefore, use of a bioreactor aids not only in endothelial attachment but in increased cell mass, collagen and elasten contents in the matrix (88).

For *in-vitro* assessment of shear stress and EC function that closely simulates physiological conditions bioreactors have been created and tested for stent evaluation (124). These can be extrapolated to studies testing the cellular

retention and function of EC re-seeded onto decellularized tissues. There is

continued controversy over the benefits of cell seeding using a perfusion

bioreactor rather than under static conditions (125). While it has been shown that

perfusion seeding has some benefit to the orientation of the ECs onto the surface

(125) there is generally no improvement in functional properties of cells reseeded

using a bioractor vs. static conditions (126).

1.4   ALLOGRAFT VS. XENOGRAFT

Xenogeneic tissues have been extensively explored for potential as donor

tissue. However, as stated above, xeno antigens expressed on the surface of these

donor tissues cause a highly active immune proliferative response (127). However

it is possible to remove these antigens via glutaraldehyde fixing (128) to attenuate

the immune assault on these tissues via cross-linking reactive antigens and

masking them from attacking immune cells, or removal of porcine gal-alpha 1

epitope (128) to decrease the inflammatory response against porcine antigens.

However, this has been shown to increase calcification of the transplanted tissues

and still suffer rejection (129). Decellularization of xenografts has had mixed

results. In 2003 the failure of the previously heralded Synergraft porcine

decellularized heart valve in pediatric patients led to the abrupt cessation of these

tissues for clinical use. The resultant valve devastation was found to be stemmed

from incomplete decellularization and cross-reactivity among the xeno antigens

(68). CryoLife has since introduced a commercially available decellularized

allograft patch for use in cardiac reconstructive surgery with promising results

and freedom from reoperation at 52 months (130), and these have been shown to

have improved durability compared to conventional allografts (131). Decellularized bovine extracellular matrix has since been shown to be well-tolerated in clinical trials with freedom from infection at 1year post-transplant (132). However, repopulation of decellularized xenografts by recipient cells remains to be shown. While glutaraldehyde treatment may prevent a foreign body inflammatory response against xenogeneic antigens, this treatment may also complicate recellularization (133). While decellularized xenografts may become a viable option for transplantation, transmission of zoonotic diseases remains a major concern. Adaptation of animal viruses in human hosts (134) raises concerns not only for the individual but for the global community, should these viruses mutate and potentially create a pandemic. Until further research addresses these concerns (135), human allograft tissues remains the best option for cardiac surgical intervention.

1.5 SUMMARY

Despite recent advancements in surgical intervention the ideal heart valve replacement still does not exist. An ideal heart valve for surgical repair would illicit a minimal immune reaction, maintain durability, resist infection, be non-thrombogenic and, most importantly in the pediatric population, have the ability to grow in proportion to the child. Human allograft tissue is commonly used to reconstruct the hearts of children with severe birth defects. Allograft tissue induces an immune response that destroys the graft and leads to allo-sensitization, complicating future transplantation. Decellularization reduces the immune response, however, acellular vascular tissue is highly thrombogenic due to loss of

endothelium. *In-vitro* endothelialization attenuates its thrombogenicity. A novel

method of cellular attachment using Arginine-Glycine-Aspartic Acid (RGD)

peptides may enhance endothelialization. This could ultimately create a custom

heart valve that may potentially grow with the child. This thesis focuses upon the

development of a method of RGD peptide attachment to a decellularized tissue

scaffold and evaluating the capacity of the RGD modified decellularized

membrane for repopulation with HUVEC cells under static conditions.

1.6 HYPOTHESIS AND THESIS AIMS:

This thesis focuses on the repopulation of decellularized ovine and allograft tissue used in cardiac surgery. It proposes to further current studies on repopulation of tissue engineered biological scaffolds by developing a method to enhance endothelial cell adhesion.

Major hypotheses to be tested include:

I. **Investigate the binding capacity of a FITC labeled RGD peptide to decellularized ovine tissue**

   Specific aims include:

   1. to evaluate the optimal mechanism of RGD peptide addition to decellularized tissue through comparison of an enzymatic addition of a maleimide ester versus spontaneous reaction of the peptide to the ECM collagen surface.

II. **Evaluate the adhesion of HUVEC cells to the RGD modified decellularized surface of ovine tissue**

   Specific aims include:

   1. determine the optimal HUVEC concentration for repopulation of decellularized tissue

2. determine the optimal time point for HUVEC cell adhesion onto decellularized tissue

3. compare HUVEC repopulation and adhesion on RGD modified versus decellularized scaffolds alone

III.   **Evaluate the reproducibility of a method for enhancing HUVEC adhesion onto RGD-modified decellularized ovine tissue into a human model**

Specific aims include:

1. replicating optimized conditions for RGD modification and HUVEC adhesion onto decellularized human allograft scaffolds

IV.   **Determine a method to remove the FITC label on our RGD peptide**

Specific aims include:

1. developing a method of enzymatic digestion for the effective removeal of the FITC label on our RGD containing peptide sequence without damaging the RGD adhesion sequence of interest
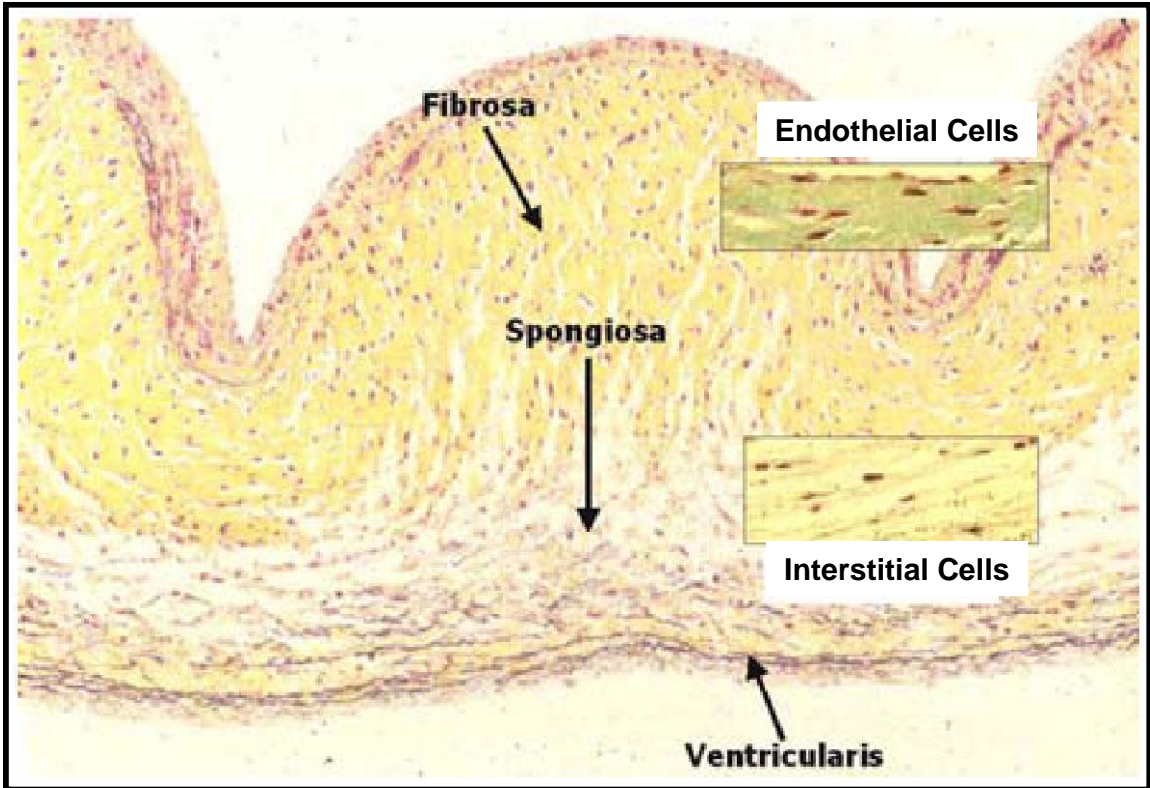
Figure 1-1. Three layers of the Extracellular Matrix (ECM). Source: Mendelson K et al. Heart Valve Tissue Engineering: Concepts, Approaches, Progress, and Challenges. 2006.
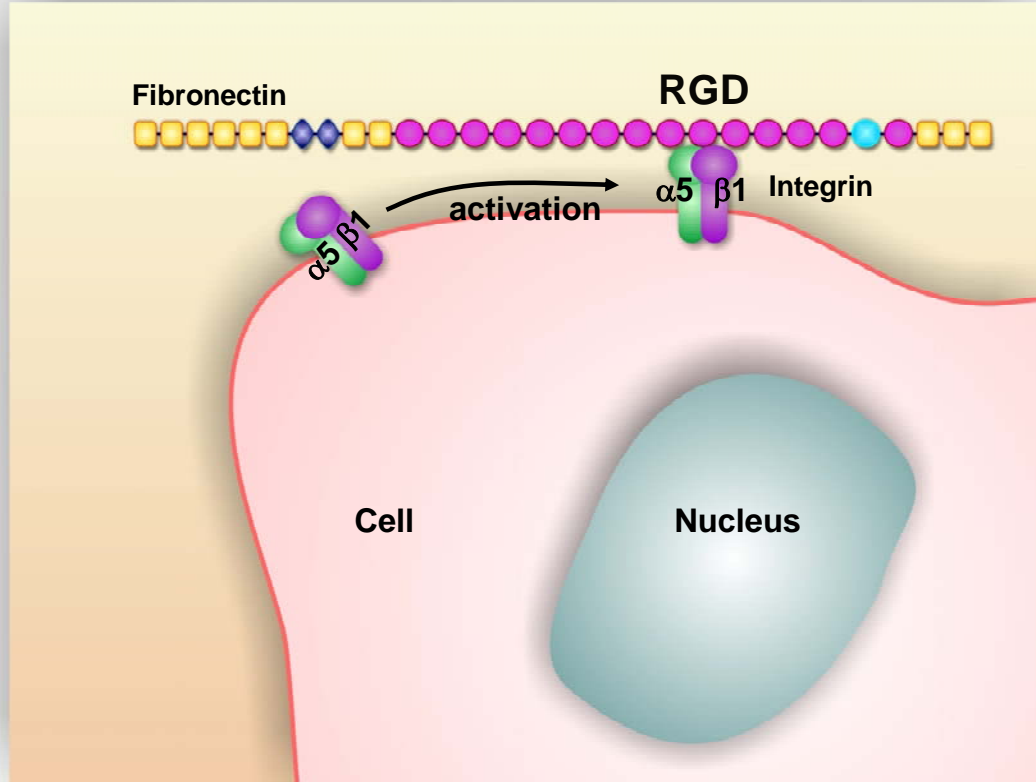
Figure 1-2. Endothelial Cell Adhesion to RGD Sequence of Fibronectin

The interaction between the RGD sequence and the α5β1 integrin receptor. The RGD sequence is contained within a 10AA subunit of FN while the integrin is present on the extracellular membrane of adherent vascular cells such as endothelial cells. Source: Theoretical and Computational Biophysics Group, University of Illinois at Urbana-Champaign.
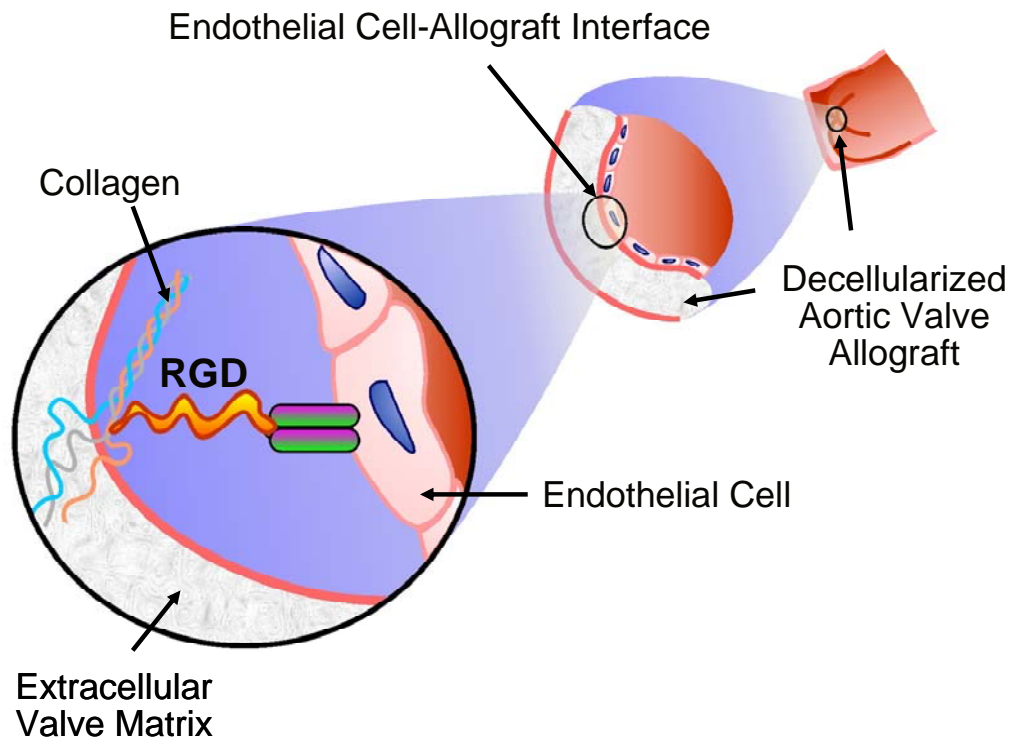
Figure 1-3. Summary of Rationale for RGD Modified Re-endothelialization

Two part hypothesis for this body of research: A: the interaction between the collagen fibres present on decellularized tissue binding to the RGD peptide of interest and B: the interaction between the RGD modified collagen surface and HUVEC endothelial cell $\alpha 5\beta 1$ integrin receptors facilitating covalent endothelialization of decellularized tissue scaffolds.

1.7   REFERENCES

1. Quader MA, Rosenthal GL, Qureshi AM, Mee RB, Mumtaz MA, Joshi R, et al. Aortic valve repair for congenital abnormalities of the aortic valve. Heart Lung Circ. 2006 Aug;15(4):248-55.

2. Jegatheeswaran A, Butany J. Pathology of infectious and inflammatory diseases in prosthetic heart valves. Cardiovasc Pathol. 2006 Sep-Oct;15(5):252-5

3. Bruck SD. Possible causes for the calcification of glutaraldehyde-treated tissue heart valves and blood contacting elastomers during prolonged use in medical devices: A physico-chemical view. Biomaterials. 1981 Jan;2(1):14-8.

4. O'Brien MF, Goldstein S, Walsh S, Black KS, Elkins R, Clarke D. The SynerGraft valve: A new acellular (nonglutaraldehyde-fixed) tissue heart valve for autologous recellularization first experimental studies before clinical implantation. Semin Thorac Cardiovasc Surg. 1999 Oct;11(4 Suppl 1):194-200.

5. Gall KL, Smith SE, Willmette CA, O'Brien MF. Allograft heart valve viability and valve-processing variables. Ann Thorac Surg. 1998 Apr;65(4):1032-8.

6. Shaddy RE, Hawkins JA. Immunology and failure of valved allografts in children. Ann Thorac Surg. 2002 Oct;74(4):1271-5.

7. Hogan PG, O'Brien MF. Improving the allograft valve: Does the immune response matter? J Thorac Cardiovasc Surg. 2003 Nov [cited 3/31/2008];126(5):1251-3.

8. Baskett RJ, Ross DB, Nanton MA, Murphy DA. Factors in the early failure of cryopreserved homograft pulmonary valves in children: Preserved immunogenicity? J Thorac Cardiovasc Surg. 1996 Nov;112(5):1170,8; discussion 1178-9.

9. Dignan R, O'Brien M, Hogan P, Thornton A, Fowler K, Byrne D, et al. Aortic valve allograft structural deterioration is associated with a subset of antibodies to human leukocyte antigens. J Heart Valve Dis. 2003 May;12(3):382,90; discussion 390-1.

10. Ascenzi JA, Kane PL. Update on complications of pediatric cardiac surgery. Crit Care Nurs Clin North Am. 2007 Dec;19(4):361,9, v.

11. Sindhi R. Sirolimus in pediatric transplant recipients. Transplant Proc. 2003 May;35(3 Suppl):113S-4S.

12. Freier MC, Babikian T, Pivonka J, Burley Aaen T, Gardner JM, Baum M, et al. A longitudinal perspective on neurodevelopmental outcome after infant cardiac transplantation. J Heart Lung Transplant. 2004 Jul;23(7):857-64.

13. Rose EA, Pepino P, Barr ML, Smith CR, Ratner AJ, Ho E, et al. Relation of HLA antibodies and graft atherosclerosis in human cardiac allograft recipients. J Heart Lung Transplant. 1992 May-Jun;11(3 Pt 2):S120-3.

14. Meyer SR, Nagendran J, Desai LS, Rayat GR, Churchill TA, Anderson CC, et al. Decellularization reduces the immune response to aortic valve allografts in the rat. J Thorac Cardiovasc Surg. 2005 Aug;130(2):469-76.

15. Wang XN, Chen CZ, Yang M, Gu YJ. Implantation of decellularized small-caliber vascular xenografts with and without surface heparin treatment. Artif Organs. 2007 Feb;31(2):99-104.

16. Kaushal S, Amiel GE, Guleserian KJ, Shapira OM, Perry T, Sutherland FW, et al. Functional small-diameter neovessels created using endothelial progenitor cells expanded ex vivo. Nat Med. 2001 Sep;7(9):1035-40.

17. Sutherland FW, Perry TE, Yu Y, Sherwood MC, Rabkin E, Masuda Y, et al. From stem cells to viable autologous semilunar heart valve. Circulation. 2005 May 31;111(21):2783-91.

18. Ingram DA, Caplice NM, Yoder MC. Unresolved questions, changing definitions, and novel paradigms for defining endothelial progenitor cells. Blood. 2005 Sep 1;106(5):1525-31.

19. Barber TA, Harbers GM, Park S, Gilbert M, Healy KE. Ligand density characterization of peptide-modified biomaterials. Biomaterials. 2005 Dec;26(34):6897-905.

20. Cohn L. Cardiac surgery in the adult (CARDIAC SURGERY IN THE ADULT). McGraw-Hill Professional; 2007.

21. Braunwald E. Mechanics and energetics of the normal and failing heart. Trans Assoc Am Physicians. 1971;84:63-94.

22. Sarris GE, Miller DC. Valvular-ventricular interaction: The importance of the mitral chordae tendineae in terms of global left ventricular systolic function. J Card Surg. 1988 Sep [cited 4/3/2008];3(3):215-34.

23. Fedak PW, McCarthy PM, Bonow RO. Evolving concepts and technologies in mitral valve repair. Circulation. 2008 Feb 19;117(7):963-74.

24. Sarris GE, Cahill PD, Hansen DE, Derby GC, Miller DC. Restoration of left ventricular systolic performance after reattachment of the mitral chordae tendineae. the importance of valvular-ventricular interaction. J Thorac Cardiovasc Surg. 1988 Jun;95(6):969-79.

25. Yun KL, Niczyporuk MA, Sarris GE, Fann JI, Miller DC. Importance of mitral subvalvular apparatus in terms of cardiac energetics and systolic mechanics in the ejecting canine heart. J Clin Invest. 1991 Jan;87(1):247-54.

26. Mendelson K, Schoen FJ. Heart valve tissue engineering: Concepts, approaches, progress, and challenges. Ann Biomed Eng. 2006 Dec;34(12):1799-819.

27. Taylor PM, Batten P, Brand NJ, Thomas PS, Yacoub MH. The cardiac valve interstitial cell. Int J Biochem Cell Biol. 2003 Feb;35(2):113-8.

28. Mulholland DL, Gotlieb AI. Cell biology of valvular interstitial cells. Can J Cardiol. 1996 Mar [cited 4/3/2008];12(3):231-6.

29. Hinton RB,Jr, Lincoln J, Deutsch GH, Osinska H, Manning PB, Benson DW, et al. Extracellular matrix remodeling and organization in developing and diseased aortic valves. Circ Res. 2006 Jun 9 [cited 3/31/2008];98(11):1431-8.

30. Butcher JT, Penrod AM, Garcia AJ, Nerem RM. Unique morphology and focal adhesion development of valvular endothelial cells in static and fluid flow environments. Arterioscler Thromb Vasc Biol. 2004 Aug;24(8):1429-34.

31. Flaherty JT, Pierce JE, Ferrans VJ, Patel DJ, Tucker WK, Fry DL. Endothelial nuclear patterns in the canine arterial tree with particular reference to hemodynamic events. Circ Res. 1972 Jan;30(1):23-33.

32. Butcher JT, Nerem RM. Valvular endothelial cells regulate the phenotype of interstitial cells in co-culture: Effects of steady shear stress. Tissue Eng. 2006 Apr [cited 3/31/2008];12(4):905-15.

33. Gomez-Cerezo JF, Pagan-Munoz B, Lopez-Rodriguez M, Estebanez-Munoz M, Barbado-Hernandez FJ. The role of endothelial progenitor cells and statins in endothelial function: A review. Cardiovasc Hematol Agents Med Chem. 2007 Oct;5(4):265-72

34. Miatton M, De Wolf D, Francois K, Thiery E, Vingerhoets G. Neurocognitive consequences of surgically corrected congenital heart defects: A review. Neuropsychol Rev. 2006 Jun;16(2):65-85.

35. Hammermeister K, Sethi GK, Henderson WG, Grover FL, Oprian C, Rahimtoola SH. Outcomes 15 years after valve replacement with a mechanical versus a bioprosthetic valve: Final report of the veterans affairs randomized trial. Journal of the American College of Cardiology,. 2000 10;36(4):1152-8.

36. Butany J, Collins MJ, Demellawy DE, Nair V, Israel N, Leong SW, et al. Morphological and clinical findings in 247 surgically excised native aortic valves. Can J Cardiol. 2005 Jul;21(9):747-55.

37. Goldbarg SH, Elmariah S, Miller MA, Fuster V. Insights into degenerative aortic valve disease. Journal of the American College of Cardiology,. 2007 9/25;50(13):1205-13.

38. Rahimtoola SH. The year in valvular heart disease. J Am Coll Cardiol. 2008 Feb 19;51(7):760-70.

39. ROSS DN. Homograft replacement of the aortic valve. Lancet. 1962 Sep 8;2(7254):487.

40. Ross DN, Somerville J. Correction of pulmonary atresia with a homograft aortic valve. Lancet. 1966 Dec 31;2(7479):1446-7.

41. Rabkin-Aikawa E, Aikawa M, Farber M, Kratz JR, Garcia-Cardena G, Kouchoukos NT, et al. Clinical pulmonary autograft valves: Pathologic evidence of adaptive remodeling in the aortic site. J Thorac Cardiovasc Surg. 2004 Oct [cited 4/3/2008];128(4):552-61.

42. Takkenberg JJ, Kappetein AP, van Herwerden LA, Witsenburg M, Van Osch-Gevers L, Bogers AJ. Pediatric autograft aortic root replacement: A prospective follow-up study. Ann Thorac Surg. 2005 Nov [cited 4/3/2008];80(5):1628-33.

43. Kadner A, Raisky O, Degandt A, Tamisier D, Bonnet D, Sidi D, et al. The ross procedure in infants and young children. Ann Thorac Surg. 2008 Mar [cited 3/31/2008];85(3):803-8.

44. Kollar A. Valve-sparing reconstruction within the native aortic root: Integrating the yacoub and the david methods. Ann Thorac Surg. 2007 Jun [cited 3/31/2008];83(6):2241-3.

45. Ruoslahti E. Fibronectin and its receptors. Annu Rev Biochem. 1988;57:375-413.

46. Hynes RO. Integrins: A family of cell surface receptors. Cell. 1987 Feb 27;48(4):549-54.

47. Jonas RA. The ross procedure is not the procedure of choice for the teenager requiring aortic valve replacement. Semin Thorac Cardiovasc Surg Pediatr Card Surg Annu. 2005:176-80.

48. Circulation 2008

49. Khan SS, Trento A, DeRobertis M, Kass RM, Sandhu M, Czer LS, et al. Twenty-year comparison of tissue and mechanical valve replacement. J Thorac Cardiovasc Surg. 2001 Aug;122(2):257-69.

50. Birkmeyer NJ, Birkmeyer JD, Tosteson AN, Grunkemeier GL, Marrin CA, O'Connor GT. Prosthetic valve type for patients undergoing aortic valve replacement: A decision analysis. Ann Thorac Surg. 2000 Dec;70(6):1946-52.

51. Pavoni D, Badano LP, Ius F, Mazzaro E, Frassani R, Gelsomino S, et al. Limited long-term durability of the cryolife O'brien stentless porcine xenograft valve. Circulation. 2007 Sep 11 [cited 3/31/2008];116(11 Suppl):I307-13.

52. Bonow RO, Carabello B, de Leon AC,Jr, Edmunds LH,Jr, Fedderly BJ, Freed MD, et al. Guidelines for the management of patients with valvular heart disease: Executive summary. A report of the american college of Cardiology/American heart association task force on practice guidelines (committee on management of patients with valvular heart disease). Circulation. 1998 Nov 3 [cited 4/2/2008];98(18):1949-84.

53. O'Brien MF, Stafford EG, Gardner MA, Pohlner PG, McGiffin DC. A comparison of aortic valve replacement with viable cryopreserved and fresh allograft valves, with a note on chromosomal studies. J Thorac Cardiovasc Surg. 1987 Dec;94(6):812-23.

54. Dittrich S, Alexi-Meskishvili VV, Yankah AC, Dahnert I, Meyer R, Hetzer R, et al. Comparison of porcine xenografts and homografts for pulmonary

valve replacement in children. Ann Thorac Surg. 2000 Sep [cited 3/31/2008];70(3):717-22.

55. Sadowski J, Kapelak B, Bartus K, Podolec P, Rudzinski P, Myrdko T, et al. Reoperation after fresh homograft replacement: 23 years' experience with 655 patients. Eur J Cardiothorac Surg. 2003 Jun [cited 3/31/2008];23(6):996,1000; discussion 1000-1.

56. Luk A, Butany J, Erlich SA, Henry J, David TE. Long-term morphological changes in a cryopreserved pulmonary valve homograft. Can J Cardiol. 2007 Aug [cited 3/31/2008];23(10):817-9.

57. Legare JF, Lee TD, Ross DB. Cryopreservation of rat aortic valves results in increased structural failure. Circulation. 2000 Nov 7;102(19 Suppl 3):III75-8.

58. Brockbank KG, Song YC. Mechanisms of bioprosthetic heart valve calcification. Transplantation. 2003 Apr 27 [cited 3/31/2008];75(8):1133-5.

59. Hogan P, Duplock L, Green M, Smith S, Gall KL, Frazer IH, et al. Human aortic valve allografts elicit a donor-specific immune response. J Thorac Cardiovasc Surg. 1996 Nov;112(5):1260,6; discussion 1266-7.

60. Legare JF, Lee TD, Creaser K, Ross DB. T lymphocytes mediate leaflet destruction and allograft aortic valve failure in rats. Ann Thorac Surg. 2000 Oct;70(4):1238-45.

61. Pompilio G, Polvani G, Piccolo G, Guarino A, Nocco A, Innocente A, et al. Six-year monitoring of the donor-specific immune response to cryopreserved aortic allograft valves: Implications with valve dysfunction. Ann Thorac Surg. 2004 Aug [cited 3/31/2008];78(2):557-63.

62. Meyer SR, Campbell PM, Rutledge JM, Halpin AM, Hawkins LE, Lakey JR, et al. Use of an allograft patch in repair of hypoplastic left heart syndrome may complicate future transplantation. Eur J Cardiothorac Surg. 2005 Apr;27(4):554-60.

63. Meyer SR, Ross DB, Forbes K, Hawkins LE, Halpin AM, Nahirniak SN, et al. Failure of prophylactic intravenous immunoglobulin to prevent sensitization to cryopreserved allograft tissue used in congenital cardiac surgery. J Thorac Cardiovasc Surg. 2007 Jun;133(6):1517-23.

64. Kasimir MT, Rieder E, Seebacher G, Silberhumer G, Wolner E, Weigel G, et al. Comparison of different decellularization procedures of porcine heart valves. Int J Artif Organs. 2003 May [cited 3/31/2008];26(5):421-7.

65. Elkins RC, Dawson PE, Goldstein S, Walsh SP, Black KS. Decellularized human valve allografts. Ann Thorac Surg. 2001 May [cited 3/31/2008];71(5 Suppl):S428-32.

66. Yacoub M, Kittle CF. Sterilization of valve homografts by antibiotic solutions. Circulation. 1970 May [cited 4/3/2008];41(5 Suppl):II29-32.

67. Meyer SR, Chiu B, Churchill TA, Zhu L, Lakey JR, Ross DB. Comparison of aortic valve allograft decellularization techniques in the rat. J Biomed Mater Res A. 2006 Nov;79(2):254-62.

68. Simon P, Kasimir MT, Seebacher G, Weigel G, Ullrich R, Salzer-Muhar U, et al. Early failure of the tissue engineered porcine heart valve SYNERGRAFT in pediatric patients. Eur J Cardiothorac Surg. 2003 Jun [cited 4/1/2008];23(6):1002,6; discussion 1006.

69. Hopkins RA, Jones AL, Wolfinbarger L, Moore MA, Bert AA, Lofland GK. Decellularization reduces calcification while improving both durability and 1-year functional results of pulmonary homograft valves in juvenile sheep. J Thorac Cardiovasc Surg. 2009 Apr;137(4):907,13, 913e1-4.

70. Seebacher G, Grasl C, Stoiber M, Rieder E, Kasimir MT, Dunkler D, et al. Biomechanical properties of decellularized porcine pulmonary valve conduits. Artif Organs. 2008 Jan;32(1):28-35.

71. Narine K, Ing EC, Cornelissen M, Desomer F, Beele H, Vanlangenhove L, et al. Readily available porcine aortic valve matrices for use in tissue valve engineering. is cryopreservation an option? Cryobiology. 2006 10;53(2):169-81.

72. Liao J, Joyce EM, Sacks MS. Effects of decellularization on the mechanical and structural properties of the porcine aortic valve leaflet. Biomaterials. 2008 Mar;29(8):1065-74.

73. Grauss RW, Hazekamp MG, van Vliet S, Gittenberger-de Groot AC, DeRuiter MC. Decellularization of rat aortic valve allografts reduces leaflet destruction and extracellular matrix remodeling. J Thorac Cardiovasc Surg. 2003 Dec [cited 3/31/2008];126(6):2003-10.

74. Vlodavsky I, Eldor A, HyAm E, Atzom R, Fuks Z. Platelet interaction with the extracellular matrix produced by cultured endothelial cells: A model to study the thrombogenicity of isolated subendothelial basal lamina. Thromb Res. 1982 Oct 15;28(2):179-91.

75. Kasimir MT, Weigel G, Sharma J, Rieder E, Seebacher G, Wolner E, et al. The decellularized porcine heart valve matrix in tissue engineering: Platelet adhesion and activation. Thromb Haemost. 2005 Sep;94(3):562-7.

76. Kasimir MT, Rieder E, Seebacher G, Nigisch A, Dekan B, Wolner E, et al. Decellularization does not eliminate thrombogenicity and inflammatory stimulation in tissue-engineered porcine heart valves. J Heart Valve Dis. 2006 Mar;15(2):278,86; discussion 286.

77. Walluscheck KP, Steinhoff G, Kelm S, Haverich A. Improved endothelial cell attachment on ePTFE vascular grafts pretreated with synthetic RGD-containing peptides. Eur J Vasc Endovasc Surg. 1996 Oct;12(3):321-30.

78. Curtil A, Pegg DE, Wilson A. Repopulation of freeze-dried porcine valves with human fibroblasts and endothelial cells. J Heart Valve Dis. 1997 May [cited 3/31/2008];6(3):296-306.

79. Takagi K, Fukunaga S, Nishi A, Shojima T, Yoshikawa K, Hori H, et al. *In-vivo* recellularization of plain decellularized xenografts with specific cell characterization in the systemic circulation: Histological and immunohistochemical study. Artif Organs. 2006 Apr;30(4):233-41.

80. Leyh RG, Wilhelmi M, Rebe P, Fischer S, Kofidis T, Haverich A, et al. *In-vivo* repopulation of xenogeneic and allogeneic acellular valve matrix conduits in the pulmonary circulation. Ann Thorac Surg. 2003 May [cited 3/31/2008];75(5):1457,63; discussion 1463.

81. Mirsadraee S, Wilcox HE, Watterson KG, Kearney JN, Hunt J, Fisher J, et al. Biocompatibility of acellular human pericardium. J Surg Res. 2007 Dec;143(2):407-14.

82. Lehr EJ, Hermary S, McKay RT, Webb DN, Abazari A, McGann LE, et al. NMR assessment of me(2)SO in decellularized cryopreserved aortic valve conduits. J Surg Res. 2007 Jul;141(1):60-7.

83. Brody S, Anilkumar T, Liliensiek S, Last JA, Murphy CJ, Pandit A. Characterizing nanoscale topography of the aortic heart valve basement membrane for tissue engineering heart valve scaffold design. Tissue Eng. 2006 Feb;12(2):413-21.

84. Rabkin-Aikawa E, Farber M, Aikawa M, Schoen FJ. Dynamic and reversible changes of interstitial cell phenotype during remodeling of cardiac valves. J Heart Valve Dis. 2004 Sep;13(5):841-7.

85. Ye X, Zhao Q, Sun X, Li H. Enhancement of mesenchymal stem cell attachment to decellularized porcine aortic valve scaffold by *in-vitro* coating with antibody against CD90: A preliminary study on antibody-modified tissue-engineered heart valve. Tissue Eng Part A. 2009 Jan;15(1):1-11.

86. Vincentelli A, Wautot F, Juthier F, Fouquet O, Corseaux D, Marechaux S, et al. *In-vivo* autologous recellularization of a tissue-engineered heart valve: Are bone marrow mesenchymal stem cells the best candidates? J Thorac Cardiovasc Surg. 2007 Aug;134(2):424-32

87. Lichtenberg A, Tudorache I, Cebotari S, Suprunov M, Tudorache G, Goerler H, et al. Preclinical testing of tissue-engineered heart valves re-endothelialized under simulated physiological conditions. Circulation. 2006 Jul 4 [cited 3/31/2008];114(1 Suppl):I559-65.

88. Schenke-Layland K, Opitz F, Gross M, Doring C, Halbhuber KJ, Schirrmeister F, et al. Complete dynamic repopulation of decellularized heart valves by application of defined physical signals-an *in-vitro* study. Cardiovasc Res. 2003 Dec 1 [cited 3/31/2008];60(3):497-509

89. Schopka S, Schmid FX, Hirt S, Birnbaum DE, Schmid C, Lehle K. Recellularization of biological heart valves with human vascular cells: *In-vitro* hemocompatibility assessment. J Biomed Mater Res B Appl Biomater. 2009 Jan;88(1):130-8.

90. Engelmayr GC,Jr, Sales VL, Mayer JE,Jr, Sacks MS. Cyclic flexure and laminar flow synergistically accelerate mesenchymal stem cell-mediated engineered tissue formation: Implications for engineered heart valve tissues. Biomaterials. 2006 Dec;27(36):6083-95.

91. Sank A, Rostami K, Weaver F, Ertl D, Yellin A, Nimni M, et al. New evidence and new hope concerning endothelial seeding of vascular grafts. Am J Surg. 1992 Sep;164(3):199-204.

92. Ingram DA, Mead LE, Tanaka H, Meade V, Fenoglio A, Mortell K, et al. Identification of a novel hierarchy of endothelial progenitor cells using human peripheral and umbilical cord blood. Blood. 2004 Nov 1;104(9):2752-60.

93. Sodian R, Lueders C, Kraemer L, Kuebler W, Shakibaei M, Reichart B, et al. Tissue engineering of autologous human heart valves using cryopreserved vascular umbilical cord cells. Ann Thorac Surg. 2006 Jun [cited 3/31/2008];81(6):2207-16.

94. Fang NT, Xie SZ, Wang SM, Gao HY, Wu CG, Pan LF. Construction of tissue-engineered heart valves by using decellularized scaffolds and endothelial progenitor cells. Chin Med J (Engl). 2007 Apr 20;120(8):696-702.

95. Schmidt D, Asmis LM, Odermatt B, Kelm J, Breymann C, Gossi M, et al. Engineered living blood vessels: Functional endothelia generated from human umbilical cord-derived progenitors. Ann Thorac Surg. 2006 Oct;82(4):1465,71; discussion 1471.

96. Raines EW. The extracellular matrix can regulate vascular cell migration, proliferation, and survival: Relationships to vascular disease. Int J Exp Pathol. 2000 Jun;81(3):173-82.

97. Mao Y, Schwarzbauer JE. Fibronectin fibrillogenesis, a cell-mediated matrix assembly process. Matrix Biol. 2005 Sep;24(6):389-99.

98. Hynes, R.O., 1990. Fibronectins. Springer-Verlag Inc., New York.

99. Ruoslahti****

100. Nagai T. A second cell recognition site of fibronectin. Seikagaku. 1991 Jul;63(7):507-12.

101. Akiyama SK. Integrins in cell adhesion and signaling. Hum Cell. 1996 Sep;9(3):181-6.

102. Pierschbacher MD, Ruoslahti E. Variants of the cell recognition site of fibronectin that retain attachment-promoting activity. Proc Natl Acad Sci U S A. 1984 Oct;81(19):5985-8.

103. McDonald JA. Extracellular matrix assembly. Annu Rev Cell Biol. 1988;4:183-207.

104. Ali, I.U., Hynes, R.O., 1978. Role of disulfide bonds in the attachment and function of large, external, transformation-sensitive glycoprotein at the cell surface. Biochim. Biophys. Acta 510, 140–150.

105. Wu C, Keivens VM, O'Toole TE, McDonald JA, Ginsberg MH. Integrin activation and cytoskeletal interaction are essential for the assembly of a fibronectin matrix. Cell. 1995 Dec 1;83(5):715-24.

106. Miyamoto S, Katz BZ, Lafrenie RM, Yamada KM. Fibronectin and integrins in cell adhesion, signaling, and morphogenesis. Ann N Y Acad Sci. 1998 Oct 23;857:119-29.

107. Briggs SL. The role of fibronectin in fibroblast migration during tissue repair. J Wound Care. 2005 Jun;14(6):284-7.

108. Dohmen PM, Lembcke A, Holinski S, Kivelitz D, Braun JP, Pruss A, et al. Mid-term clinical results using a tissue-engineered pulmonary valve to reconstruct the right ventricular outflow tract during the ross procedure. Ann Thorac Surg. 2007 Sep;84(3):729-36.

109. Johnson KJ, Sage H, Briscoe G, Erickson HP. The compact conformation of fibronectin is determined by intramolecular ionic interactions. J Biol Chem. 1999 May 28;274(22):15473-9.

110. Sechler JL, Corbett SA, Wenk MB, Schwarzbauer JE. Modulation of cell-extracellular matrix interactions. Ann N Y Acad Sci. 1998 Oct 23;857:143-54.

111. Iop L, Renier V, Naso F, Piccoli M, Bonetti A, Gandaglia A, et al. The influence of heart valve leaflet matrix characteristics on the interaction between human mesenchymal stem cells and decellularized scaffolds. Biomaterials. 2009 May 27.

112. Sechler JL, Takada Y, Schwarzbauer JE. Altered rate of fibronectin matrix assembly by deletion of the first type III repeats. J Cell Biol. 1996 Jul;134(2):573-83.

113. Pierschbacher MD, Ruoslahti E. Cell attachment activity of fibronectin can be duplicated by small synthetic fragments of the molecule. Nature. 1984 May 3-9;309(5963):30-3.

114. Stile RA, Shull KR, Healy KE. Axisymmetric adhesion test to examine the interfacial interactions between biologically-modified networks and models of the extracellular matrix. Langmuir. 2003;19(5):1853-60.

115. Fussell GW, Cooper SL. Endothelial cell adhesion on RGD-containing methacrylate terpolymers. J Biomed Mater Res A. 2004 Aug 1;70(2):265-73.

116. Lin HB, Garcia-Echeverria C, Asakura S, Sun W, Mosher DF, Cooper SL. Endothelial cell adhesion on polyurethanes containing covalently attached RGD-peptides. Biomaterials. 1992;13(13):905-14.

117. Xiao Y, Truskey GA. Effect of receptor-ligand affinity on the strength of endothelial cell adhesion. Biophys J. 1996 Nov;71(5):2869-84.

118. Reinhart-King CA, Dembo M, Hammer DA. Endothelial cell traction forces on RGD-derivatized polyacrylamide substrata. Langmuir. 2003;19(5):1573-9.

119. Kim S, Chung EH, Gilbert M, Healy KE. Synthetic MMP-13 degradable ECMs based on poly(N-isopropylacrylamide-co-acrylic acid) semi-interpenetrating polymer networks. I. degradation and cell migration. J Biomed Mater Res A. 2005 Oct 1;75(1):73-88.

120. Boyer B, Kern P, Fourtanier A, Labat-Robert J. Age-dependent variations of the biosyntheses of fibronectin and fibrous collagens in mouse skin. Exp Gerontol. 1991;26(4):375-83.

121. Ingber DE. Tensegrity: The architectural basis of cellular mechanotransduction. Annu Rev Physiol. 1997;59:575-99.

122. Meinhart JG, Schense JC, Schima H, Gorlitzer M, Hubbell JA, Deutsch M, et al. Enhanced endothelial cell retention on shear-stressed synthetic vascular grafts precoated with RGD-cross-linked fibrin. Tissue Eng. 2005 May-Jun;11(5-6):887-95.

123. Wu YF, Zhang J, Gu YQ, Li JX, Wang LC, Wang ZG. Reendothelialization of tubular scaffolds by sedimentary and rotative forces: A first step toward tissue-engineered venous graft. Cardiovasc Revasc Med. 2008 Oct-Dec;9(4):238-47.

124. Punchard MA, O'Cearbhaill ED, Mackle JN, McHugh PE, Smith TJ, Stenson-Cox C, et al. Evaluation of human endothelial cells post stent deployment in a cardiovascular simulator *in-vitro*. Ann Biomed Eng. 2009 Apr 30.

125. Au-Yeung KL, Sze K, Sham MH, Chan BP. Development of a micromanipulator-based loading device for mechanoregulation study of human mesenchymal stem cells in 3D collagen constructs. Tissue Eng Part C Methods. 2009 Apr 15.

126. Brown MA, Iyer RK, Radisic M. Pulsatile perfusion bioreactor for cardiac tissue engineering. Biotechnol Prog. 2008 Jul-Aug;24(4):907-20.

127. Cowan PJ, d'Apice AJ. Complement activation and coagulation in xenotransplantation. Immunol Cell Biol. 2009 Mar-Apr;87(3):203-8.

128. Kasimir MT, Rieder E, Seebacher G, Nigisch A, Dekan B, Wolner E, et al. Decellularization does not eliminate thrombogenicity and inflammatory stimulation in tissue-engineered porcine heart valves. J Heart Valve Dis. 2006 Mar;15(2):278,86; discussion 286.

129. Manji RA, Zhu LF, Nijjar NK, Rayner DC, Korbutt GS, Churchill TA, et al. Glutaraldehyde-fixed bioprosthetic heart valve conduits calcify and fail from xenograft rejection. Circulation. 2006 Jul 25;114(4):318-27.

130. Bechtel JF, Stierle U, Sievers HH. Fifty-two months' mean follow up of decellularized SynerGraft-treated pulmonary valve allografts. J Heart Valve Dis. 2008 Jan;17(1):98,104; discussion 104.

131. Tavakkol Z, Gelehrter S, Goldberg CS, Bove EL, Devaney EJ, Ohye RG. Superior durability of SynerGraft pulmonary allografts compared with standard cryopreserved allografts. Ann Thorac Surg. 2005 Nov;80(5):1610-4.

132. Chemla ES, Morsy M. Randomized clinical trial comparing decellularized bovine ureter with expanded polytetrafluoroethylene for vascular access. Br J Surg. 2009 Jan;96(1):34-9.

133. Rieder E, Nigisch A, Dekan B, Kasimir MT, Muhlbacher F, Wolner E, et al. Granulocyte-based immune response against decellularized or glutaraldehyde cross-linked vascular tissue. Biomaterials. 2006 Nov;27(33):5634-42.

134. Boneva RS, Folks TM. Xenotransplantation and risks of zoonotic infections. Ann Med. 2004;36(7):504-17.

135. Dorling A. Clinical xenotransplantation: Pigs might fly? Am J Transplant. 2002 Sep;2(8):695-700.

2   RE-ENDOTHELIALIZATION OF DECELLULARIZED HEART TISSUE

2.1   INTRODUCTION:

With a worldwide incidence of 0.6%, congenital heart disease poses a significant health concern (1). The number of children requiring surgical intervention is roughly 0.3 to 1% of cases, in western countries (2). Due to advances in surgical training and outcomes there is a growing trend toward surgical treatment versus palliative care (3). Surgical reconstruction of major blood vessels is the most common procedure. As a result, there is an increasing need for an ideal transplantable tissue. An ideal tissue for surgical repair would illicit a minimal immune reaction, maintain durability, resist infection, be non-thrombogenic and, most importantly in the pediatric population, have the ability to grow in proportion to the child (4).

Clinical Perspective:

Despite recent advancements in congenital surgery both in surgical practice and, importantly, is surgical research, the ideal transplantable cardiac tissue for use in repair cardiac defects still does not exist. While synthetic and xenogeneic alternatives have been explored to counteract the deficit of allograft tissue, the associated limitations of these types of materials including infection and loss of durability render them substandard to human allograft tissues. While allograft tissue is considered the gold standard for surgical repair, these tissues may become damaged after cryopreservation, or infected (5) compromising the recipient after surgery. In addition current cryopreservation methods, which

preserve allogeneic cellular components of the tissue, result in a widespread immune and inflammatory reaction in the host which impairs valve function through deterioration of the donor tissue (7,8). The cell-mediated immune response is well documented in the literature and results in increased fibrosis and degeneration of valve leaflets and ECM (9). This has serious implications for patients who suffer from failed or rejected transplants and must undergo further surgeries to correct this. Future surgeries are associated with an increased risk of mortality and morbidity (3). In addition to the cell mediated immune attack is a buildup of alloreactive antibodies in the host which can complicate future transplantations through accelerated rejection of the subsequent transplant (10).

Tissue engineering endeavours such as decellularization of these immunogenic tissues has been shown *in-vivo* to drastically reduce both the cell mediated and humoral immune responses to these valves. Unfortunately, due to removal of cellular components, including the necessary endothelium, decellularized tissues are associated with an increased thrombogenicity *in-vivo* (6). *In-vitro* re-endothelialization of decellularized scaffolds prior to implantation can reduce this associated thrombogenicity (11,12).

To the best of our knowledge, no group has shown adequate retention of an *in-vitro* endothelium in an *in-vivo* model. Endothelial cells simply attached to tissue *in-vitro* are sloughed off due to shear stress in an *in-vivo* model (13). The current research initiative was to find an effective method to re-endothelialize the surface of decellularized tissue and facilitate retention of the neoendothelium *in-vivo*. RGD peptides are known to be important in facilitating endothelial cell

53

binding. (14,15) via cell surface integrin receptors (16). A novel method of attachment using RGD ligand peptides may covalently bind endothelial cells to the surface of decellularized tissue and enhance cellular retention *in-vivo*.

While xenotransplantation benefits from increasing literature expounding its potential for overcoming the human allograft donor shortage of transplantable tissues, more studies are required before xenografts become the gold standard for surgical repair. Thus, human allograft tissues remain the best choice for cardiac repair of congenital defects (5). While many tissue engineering studies focus upon recellularization of porcine or ovine decellularized valves, few studies focus upon the translateability of these results to human tissue. It will be important to show recellularization *in-vitro* using human tissues in order to reliably extrapolate the basic science research of recellularization to a clinical model.

By using the patients' own endothelial cells to repopulate a decellularized valve, a custom heart valve could potentially be available. In addition, this valve may have the potential to grow, leading to a non-immunogenic custom heart valve replacement that could endure for the patients' entire life and eliminate the need for re-transplantation later in life.

The aim of this study is to determine whether endothelialization of decellularized tissue scaffolds can be increased using a known endothelial cell adhesion ligand RGD peptide fluorescently labeled with a FITC probe. First, a method to bind the RGD-FITC peptide to the decellularized scaffold will be determined and then optimal HUVEC cell concentration necessary to begin repopulation will be assessed. Assessment of the extent of re-endothelialization

and any subsequent benefit from the use of RGD peptides will be examined via histological staining, immunofluorescence imaging, confocal imaging and DNA quantification.

2.2 METHODS

2.2.1 DECELLULARIZATION

Our method of decellularization has been described previously (6); however longer incubation times were performed here to ensure removal of cellular debris. In brief, cryopreserved juvenile Suffolk sheep pulmonary arteries (17) or cryopreserved human aorta (Comprehensive Tissue Center, University of Alberta) conduits were thawed in a 37ºC water bath for ~10 minutes. The tissue was rinsed briefly in PBS and then placed into CMRL solution (90mL, Gibco), fetal bovine serum (FBS; 10mL, Sigma) and penicillin-streptomycin solution (penstrep; 0.5mL, Sigma) for 24 hours at 4ºC. Tissue was transferred to 100mL of hypotonic Tris buffered solution (10mM, pH 8.0, 0.1mM PMSF, 5mM EDTA) for 72 hours. The hypotonic solution was then replaced with hypertonic Tris buffered solution (50mM, pH 8.0, 1.5M KCl, 5mM EDTA) containing 0.5% Triton-X-100 (Labchem Inc, Pittsburgh, PA, USA) again for 72 hours at 4ºC. A 5 hour rinse with Sorensen's buffer containing DNAse (25mg/mL, Roche, Laval, QC, Canada), RNAse (10g/mL, Roche, Laval, QC, Canada) and MgCl$_2$ (10mmol/L) was performed at 37ºC followed by a washout in Tris buffer (50mM, pH 9.0) with 0.5% Triton X-100 for 72 hours at 4ºC. Tissues were soaked in PBS for 72 hours and then stored in CMRL (90mL), FBS (10mL) and penstrep (0.5mL) at 4ºC. All steps were performed with constant stirring. Histological assessment with haematoxylin-eosin staining assessed decellularization.

2.2.2 RGD FUNCTIONALIZATION ONTO DECELLULARIZED OVINE TISSUE

Our method of RGD functionalization onto decellularized tissue is

modified from Stile et al (18) (Figure 2-1). 30mm disks were dissected out of

decellularized patches of ovine tissue using a standard one-hole punch. 24 disks

were placed into a fluorescent 96-well plate and washed once with 100µL PBS

and once with 100µL ultrapure water (UPW) and disks were resuspended in

UPW. Basal auto fluorescence was measured using a fluorometer (428mm

Fluoroskan Ascent). The UPW was aspirated and replaced with either 100µL

fresh UPW (Group 1), 100µL 2-[morpholino]ethanesulfonic acid (MES) buffer

(0.1M, pH 6.5, Rock Pierce, Il) (Group 2) or 100µL MES buffer (0.1M, pH 6.0)

with 1-Ethyl-3-[3-dimethylaminopropyl]carbodiimide hydrochloride (EDC)

(3.9mg/mL, Rock Pierce, Il), N-hydroxysulfosuccinimide (sulfo-NHS)

(1.1mg/mL, Rock Pierce, Il) and our maleimide group of interest [N-e-

Maleimidocaproic acid] hydrazide (EMCH) (0.5mg/mL, Rock Pierce, Il) (Group

3 and 4). Group 1 and 2 after the addition of EMCH were negative controls for

the EMCH addition. Disks in the 96-well plate were shaken at room temperature

for 2 hours on a plate shaker. Byproducts and unreacted components were

removed by aspiration and disks were washed in 100µL of 0.1M MES buffer (pH

6.5) three times followed by a wash in 100µL UPW. Disks were suspended in

100µL of 0.1M sodium phosphate buffer (pH 6.6) and fluorescence was

measured. The sodium phosphate buffer was then aspirated and replaced with a

commercially purchased peptide RGD-FITC (10µM, Ac-

CGGNGEPRGDTYRAYK(FITC)G-NH2, American Peptide Company) in disks

of Group 1, 2 and 3. Group 4 was suspended in phosphate buffer alone as a negative control for RGD-FITC addition. The reaction was allowed to proceed for 2 hours at room temperature on a plate shaker. Byproducts and unreacted peptide were again removed by aspiration and washed twice with 100µL sodium phosphate buffer, then further washed 4 times with 100µL PBS and finally suspended in 100µL of UPW and final fluorescence measures were taken.

2.2.3 HUVEC CELL PREPARATION

A commercial cell line was purchased from Lonza Cells. The protocol for cell culture and harvesting can be found on the Lonza website (www.lonza.com). In brief, stock cells were thawed and placed into T-75 tissue culture treated flasks (Beckton-Dickinson) with 15mL pre-warmed supplemented basal media and placed in a 37ºC incubator and allowed to grow to confluence. Media was changed every other day. Upon ~80% confluence cells were harvested using commercially purchased reagents. Media was aspirated from the flasks and 15mL HEPES-BSS (Lonza) was used to wash away excess protein that would inactivate trypsin. 6mL trypsin (Lonza) per flask for 2 ½ minutes was followed by 12mL of trypsin neutralizing solution (TNS, Lonza). Harvested cells were collected and centrifuged at 230g x 6 minutes and resuspended in 10mL room temperature culture media. Cells were counted using a hemocytometer and trypan blue exclusion dye and either replated into new T-75 culture flasks or used for experimental purposes. While Lonza states that HUVECs are identified by morphology alone, we stained HUVECs for anti-CD31 (CD31-FITC, AbCAM), anti-VonWillebrand Factor (VWF, AbCAM) and anti-vascular endothelial growth

factor receptor 2 (VEGFR2, AbCAM); all known endothelial cell markers.

2.2.4 HUVEC-RGD BINDING AFFINITY

1 x 10^6 HUVECs were incubated with either 100ul of 10μM or 50M

RGD-FITC for 2 hours in basal media. Cells were fixed in 1% formaldehyde for

30minutes at 4ºC then spun at 230g for 5 minutes. Wells were aspirated and

washed twice with FACS buffer (1%FBS in PBS). Cells were resuspended in

50μL of FACS buffer, mixed, transferred to a 5mL tube, 300μL of FACS buffer

was added to each tube and the cells analyzed by flow cytometry (BD Facs-

Calibur). Positive cell binding to RGD-FITC was indicated by a rightward shift.

2.2.5 HUVEC CELL BINDING TO RGD FUNCTIONALIZED DECELLULARIZED OVINE TISSUE

30mm disks were dissected out of decellularized patches of ovine tissue.

36 disks were placed into a 96-well plate and washed once with 100μL PBS and

once with 100μL ultrapure water (UPW) and disks were resuspended in UPW.

Basal auto fluorescence was measured using a fluorometer. The UPW was then

aspirated and 18 disks were suspended in 100μL sodium phosphate buffer alone

(control) and 18 disks were suspended in 100μL RGD-FITC (50μM, American

Peptide Company). The reaction was allowed to proceed for 2 hours at room

temperature on a plate shaker. Byproducts and unreacted peptide were removed

by aspiration and washed twice with 100μL sodium phosphate buffer, then further

washed 4 times with 100μL PBS and finally suspended in 100μL of UPW and

final fluorescence measures were taken.

HUVEC cells were cultured at 80% confluence and viable cells counted

on a hemocytometer using trypan-blue exclusion dye. Cells were resuspended at

concentrations of 1×10^4, 1×10^5 and 1×10^6 cells per 100µL and each concentration was added to Group 1 (control) and Group 2 (RGD-FITC) at each an n=6. An extra 100µL of supplemented HUVEC media was added to each well and the 96-well plate placed into an incubator. Disks were extracted in duplicate at time 36 hours, 3 days and 8 days for both control and RGD-FITC modified groups. Samples were formalin fixed (10%), paraffin embedded, serially sectioned and stained with H&E for histologic examination.

2.2.6 IMMUNOFLUORESCENCE STAINING

To ensure that all cells visualized with H&E staining were HUVEC and not remnant from native tissue, immunofluorescence staining for CD31 (rabbit anti-human, Abcam) was conducted on experimental slides of RGD-modified recellularized decellularized disks. Native sheep pulmonary artery, decellularized sheep pulmonary artery and single-cell suspensions of HUVECs were likewise stained with anti CD31 antibody as controls. In brief, unstained paraffin embedded slides, each with two tissue sections per slide, were rehydrated, and antigen retrieval using citrate buffer was performed. After briefly soaking in PBS, both tissue sections on each slide were outlined and blocked with normal goat serum (NGS) for 15 minutes, after which primary antibody (rabbit anti CD31, AbCam) was added to only one tissue section per slide. After 45 minutes incubation at room temperature slides underwent 3 quick washes in PBS. Secondary antibody (anti rabbit Alexa 594, Invitrogen) was added to the sections that were treated with primary antibody and to the sections that had not been incubated with primary antibody. The secondary alone sections were used as

controls for any non-specific secondary antibody staining. After a 25 minute

incubation in the dark at room temperature and subsequent rinses with PBS the

slides were coverslipped manually with DAPI nucleus stain (Prolong Gold

Antifade, Invitrogen) and left to dry overnight in the dark at room temperature.

Slides were examined under an inverted fluorescent microscope using rhodamine,

FITC and DAPI fluorescent filters.

2.2.7 CONFOCAL IMAGING

Confocal microscopy was used to visualize the density of HUVEC binding to the

decellularized surface. 30mm disks were cut from decellularized sheep

pulmonary artery and either modified with RGD-FITC as per the above stated

experimental protocol or incubated with buffer alone as controls (n=2 each

group). After confirmation of RGD-FITC labeling, fluorescently labeled HUVEC

cells (Qtracker Red, Molecular Probes) were seeded onto the disks at a

concentration of 1×10^6 cells/disk and incubated at 37º for 3 days. Media was

changed after 2 days of incubation. Surfaces were not washed prior to viewing on

the microscope. A Zeiss 510 LSM confocal microscope was used to visualize the

endothelial cell adhesion pattern on the modified surfaces. DAPI dye was added

just prior to examination under the microscope.

2.2.8 DNA ANALYSIS OF RECELLULARIZED OVINE TISSUE

Quantitative analysis of RGD dependent recellularization utilizing a

fluorescent nucleic acid stain to measure double stranded DNA was performed

using a Pico-Green standard DNA assay (Molecular Probes). 30mm disks were

cut from decellularized sheep pulmonary artery and either modified with RGD-

FITC or incubated with buffer alone as previously described. Duplicates of decellularized tissue alone, decellularized tissue with 1×10^6 HUVECs/disk or RGD-FITC modified decellularized tissue with 1×10^6 HUVECs/disk were incubated at 37ºC for 3 days. Media was changed after 2 days and frozen at -20ºC. On the third day, tissues were extracted, and frozen at -20ºC overnight. The remaining media in the incubation plates was also frozen at -20ºC. For DNA content, aliquots were washed in citrate buffer (150 mmol/liter NaCl, 15 mmol/liter citrate, 3 mmol/liter EDTA, pH 7.4). Before being assayed, cell pellets were placed in 1ml of lysis buffer (10 mmol/liter Tris, 1 mmol/liter EDTA, 0.5% Triton X-100, 4ºC, pH 7.5), sonicated, vortexed, and incubated at 65 and 70ºC for 45 and 10 min, respectively. Lysates were supplemented with 25ml of RNase A solution (10 mg/ml), vortexed,and incubated for 1 h at 37ºC. Aliquots of 25 and 50ml were assayed in duplicate by diluting them in 1 ml of DNA buffer (10 mmol/liter Tris, 1 mmol/liter EDTA, pH 7.5) and measuring fluorescence at 490 exc. / 515 em. nm (Fluoroskan Ascent) after the addition of 1 ml of Pico Green reagent (1/200 dilution with DNA buffer). Samples were run in parallel with and diluted in proportion to a seven point (0–400 ng/ml) standard curve which was generated using calf thymus DNA.

2.2.9 RGD FUNCTIONALIZATION ONTO DECELLULARIZED HUMAN TISSUE

The method for RGD functionalization onto decellularized human tissue follows the same as for ovine tissue elaborated upon earlier. 24 disks were cut from human decellularized aorta and randomly allocated to 4 groups as previously described. Fluorescence measures at basal, after EMCH addition and after 50µM

61

RGD-FITC addition were taken and compared to determine if the EMCH reaction was necessary for human tissue RGD modification.

2.2.10 HUVEC CELL BINDING TO RGD FUNCTIONALIZED DECELLULARIZED HUMAN TISSUE

30mm disks were dissected out of decellularized patches of human tissue. 6 disks were placed into a 96-well plate and washed once with 100µL PBS and once with 100µL ultrapure water (UPW) and disks were resuspended in UPW. Basal auto fluorescence was measured using a fluorometer. The UPW was then aspirated and 4 disks were suspended in 100µL sodium phosphate buffer alone (control) and 2 disks were suspended in 100µL RGD-FITC (50µM, American Peptide Company). The reaction was allowed to proceed for 2 hours at room temperature on a plate shaker. Byproducts and unreacted peptide were removed by aspiration and washed twice with 100µL sodium phosphate buffer, then further washed 4 times with 100µL PBS and finally suspended in 100µL of UPW and final fluorescence measures were taken.

HUVEC cells were cultured at 80% confluence and viable cells counted on a hemocytometer using trypan-blue exclusion dye. Cells were resuspended at concentrations of $1x10^6$ cells per 100µL and each concentration was added to Group 2 (control) and Group 3 (RGD-FITC) at each an n=2. Group 1 was a negative control for HUVEC cell addition. An extra 100µL of supplemented HUVEC media was added to each well and the 96-well plate placed into an incubator. Disks were extracted in duplicate at time 3 days for all three groups. Samples were formalin fixed (10%), paraffin embedded, serially sectioned and stained with H&E for histologic examination.

2.2.11 DNA ANALYSIS OF RECELLULARIZED HUMAN TISSUE

Refer to DNA analysis methodology for ovine tissue. Methods were

repeated using 6 disks of human decellularized aorta and HUVEC groups were

seeded with 1×10^6 cells for 3 days under static conditions.

2.2.12 RGD DIGESTION

Our methods for FITC cleavage is adapted from Barber et. al. In brief, a

10 μm solution of the custom peptide, RGD-FITC, was prepared in a 25 mm

Ammonium Bicarbonate buffer (100 mm CaCl2, pH=8.0). High-purity

chymotrypsin from bovine pancreas (21,500 g/mol, in 0.9% NaCl in water,

Calbiochem, San Diego, CA) was then added to the peptide solution in a 1:50

(vol:vol) ratio. The final activity of the solution was 1496 U/mL (one unit (U) is

the amount of enzyme that causes a 0.0075 decrease in absorbance at 237 nm,

using N-acetyl-l-tyrosine ethyl ester (25 °C, pH=7.0)). The reaction was allowed

to go to completion overnight at 37º C. Both digested and undigested controls

were reduced using 0.8mg/mL of dithiothreitol (DTT, Fisher Scientific) to prevent

dimerization.

2.2.13 RGD CHARACTERIZATION

Samples and undigested controls were separated using an Agilent 1100

HPLC system (Agilent, Palo Alto, CA) equipped with an Eclipse XDB-C8

column (Agilent). Samples were injected in ultrapure water (ASTM grade I water,

18.2 MΩ resistance) (UPW) containing 0.1% trifluoroacetic acid (TFA) and

equilibrated for 5 min, followed by elution in a linear acetonitrile (with 0.1%

TFA) gradient (0–40% over 35 min). Major eluted peaks were collected and run

through mass spectrometry analysis and compared to a table of predicted peptide

fragments determined using a proteolysis simulator (Table 2-1) (18).

2.2.14 STATISTICAL ANALYSIS

Fluorescence values are expressed as mean relative fluorescent units

(RFUs) ± standard deviation. Non-parametric analysis of variance testing

(Kruskal-Wallis) was used to compare multiple groups with Tukey's post hoc

analysis to compare individual groups. A Mann-Whitney non-parametric t-test

was used to compare two groups.

2.3   RESULTS:

2.3.1   RGD FUNCTIONALIZATION ONTO DECELLULARIZED TISSUE

Decellularization was confirmed by the absence of haematoxylin staining

indicating successful removal of cellular components (Figure 2-2). Fluorescence

data are summarized in Figure 2-3. Basal measures of fluorescence showed some

decellularized tissue auto fluorescence for all 24 disks, however, there was no

significant difference in auto fluorescence among the four groups (12.94 ± 1.16,

11.84 ± 0.57, 11.40 ± 2.51, 10.77 ± 1.61; $p=0.11$). The enzymatic addition of EMCH

showed low corrected fluorescence in the negative control groups 1 and 2 with

significance between both of these two groups and group 3 that had EMCH

(4.08 ± 3.38, 4.16 ± 3.67, 11.62 ± 3.53; $p<0.05$). No significance was found,

however, between groups 1 and 2 and group 4 (4.08 ± 3.38, 4.16 ± 3.67, 6.82 ± 2.47;

$p>0.05$) which also had EMCH or between groups 3 and 4 (11.62 ± 3.53,

6.82 ± 2.47; $p>0.05$). When RGD-FITC was added to groups 1, 2 and 3, all three

exhibited a significant difference compared to group 4 (1198 ± 155.7, 1269 ± 262.8,

1226±210.3, 11.07±5.18; p<0.0001). No significant difference was detected between the three RGD-FITC treated groups indicating no need for the extra EMCH step (Figure 2-3).

2.3.2   HUVEC CELL CHARACTERIZATION

Morphological analysis at ~80% confluency confirmed HUVEC cells. In addition, flow kilometric mean fluorescence intensity was used to quantify anti-CD31 (70.2%; n=10000), anti-VWF (87.2%; n=10000) and anti-VEGFR2 (47.6%; n=10000) staining, showing a positive indication of endothelial cell markers and function (Figure 2-4).

2.3.3   HUVEC RGD BINDING AFFINITY

Flow kilometric mean fluorescence intensity showed 58.5% (n=10000) of gated cells bound to 10μM RGD-FITC (Figure 2-4). This binding was increased to 96.4% (n=10000) with 50μM RGD-FITC making 50μM the ideal RGD-FITC concentration for subsequent HUVEC binding experiments.

2.3.4   HUVEC BINDING TO RGD FUNCTIONALIZED DECELLULARIZED TISSUE

Basal measures of fluorescence showed some decellularized tissue auto fluorescence for all 36 disks. The auto fluorescence was found to be significant between the control and the RGD-FITC groups (36.40±9.33 vs. 44.44±9.85; p=0.024). However, after RGD-FITC addition to group 2 the difference between group 1 and group 2 became very significant (35.57±10.23 vs. 3707±503.4; p<0.0001) (Figure 2-5).

Representative sections of disks extracted at 36 hours, 3 and 8 days are shown in Figure 2-6. Most notable in these images is the increased cell migration to the

basement membrane of both control tissue and RGD functionalized tissue for

$1x10^6$ cells compared to $1x10^4$ and $1x10^5$ cells for both RGD and no RGD disks.

RGD functionalized tissue appears to promote cell migration to the endothelial

surface compared to control tissue at this concentration. Disks extracted at 3 days

post HUVEC incubation with $1x10^6$ cells show a similarly higher cell layer

compared to $1x10^4$ and $1x10^5$ cell concentrations for both control and RGD

groups. In addition, at day 3 HUVECs appear to be adherent to the endothelial

surface with an increased monolayer formed on the RGD functionalized surface

compared to the control. Day 8 histology shows decreased HUVEC adhesion

compared to day 3 sections.

2.3.5   IMMUNOFLUORESCENCE STAINING

Representative photomicrographs of immunofluorescence staining of

native ovine tissue, decellularized ovine tissue, control single-cell suspension of

HUVECs and experimental HUVEC bound RGD functionalized decellularized

ovine tissue are presented in Figure 2-7. As seen, decellularized tissue showed

significantly less DAPI nuclei staining as well as CD31 staining confirming

complete decellularization of the ovine tissue. HUVECs are seen to have

significant autofluorescence as seen under the FITC filter. This autofluorescence

was also seen in the HUVECs bound in our experimental slide. Tissue

autofluorescence was also seen with both rhodamine and FITC filters, however,

there is an increase in the FITC signal after RGD modification compared to native

and decellularized ovine tissue.

2.3.6 CONFOCAL IMAGING

HUVECs bound to the surface of RGD modified and non-RGD modified decellularized tissue were seen to be evenly distributed over the entire surface area (Figure 2-8). Increased HUVECs were visible on the RGD modified tissue using DAPI staining. In addition, some evidence of native peaks and valley topography of the ECM surface is shown through FITC signal.

2.3.7 DNA ANALYSIS OF RECELLULARIZED OVINE TISSUE

Calculated DNA content per sample is shown in Figure 2-9. DNA content, measured in ng/disk were not found to be statistically significant among the three groups of decellularized tissue alone, decellularized tissue incubated with HUVECs and RGD-FITC modified decellularized tissue incubated with HUVECs (1.66 ± 1.57, 274.0 ± 4.00, 623.9 ± 20.29; $p=0.102$) however, higher levels of DNA content were seen in the RGD-FITC modified HUVEC group.

2.3.8 RGD FUNCTIONALIZATION ONTO DECELLULARIZED HUMAN TISSUE

Fluorescence data for the RGD functionalization onto decellularized human tissue is shown in Figure 2-10. Basal fluorescence showed increased human tissue autofluorescence compared to ovine, however, there was no significant difference in auto fluorescence among the four groups (91.37 ± 7.82, 99.61 ± 3.92, 93.48 ± 11.18, 98.51 ± 1.44; $p=0.644$). The enzymatic addition of EMCH to human tissue showed the same pattern as on ovine tissue, with significance between both negative control groups (Water alone and MES buffer alone) compared to the first EMCH group (1.69 ± 6.31, 0.03 ± 10.02, 33.72 ± 9.79, $p<0.05$). There was no significant difference between the negative control groups

and the second EMCH group (17.71±7.33; p>0.05), nor between the two EMCH groups. When RGD-FITC was added to the first three groups all three exhibited an increased fluorescence compared to group 4 which did not receive any peptide, however, this increase in fluorescence was not found to be statistically significant (1993±167.6, 1933±218.3, 2088±183.8, 18.77±9.63; p=0.066). There was no significant difference detected between the three RGD-FITC treated groups, thus the EMCH addition is also not necessary in decellularized human tissue modification with RGD-FITC.

2.3.9 HUVEC CELL BINDING TO RGD FUNCTIONALIZED DECELLULARIZED HUMAN TISSUE

Basal measures of fluorescence showed high tissue auto fluorescence for all 12 disks. The auto fluorescence was not significantly different amongst the three groups (115.6±8.70, 106.4±8.40, 114.5±3.39; p=0.65). Interestingly, after RGD-FITC addition to Group 3, the difference between all three groups was also not found to be statistically significant after correction for tissue basal fluorescence (8.22±2.33, 7.17±16.18, 1609±249.8; p=0.18) (Figure 11). Histologic sections at day 3 indicate a similar cell adhesion pattern to that seen with ovine tissue (Figure 2-12). Increased HUVEC binding on RGD modified surfaces compared to non-modified surfaces is seen.

2.3.10 DNA ANALYSIS OF RECELLULARIZED HUMAN TISSUE

Average DNA content per treatment group is observed in Figure 2-13. Measures of DNA in ng/sample followed the same pattern of DNA content as seen in ovine tissue and were likewise not found to be statistically significant among groups (16.31±0.50, 319.8±110.4, 550.8±148.6; p=0.102).

2.3.11 RGD CHARACTERIZATION

The predicted value of 2288.9 g/mol molecular weight for the RGD-FITC laeled 18 AA peptide was confirmed with mass spectrometry. The control peptide eluted out of the HPLC column at 26.2 minutes (Figure 2-14) and contained a significantly higher proportion of the undamaged peptide at 2289.1 m/z (Figure 2-15). A small fraction of the peptide was present without the FITC label at 1899.9 m/z. No dimerization of the peptide was seen in the controls indicating successful reduction of thiol groups using DTT. The HPLC fractions and corresponding peptide fragments detected are summarized in Table 2-1.

2.3.12 RGD DIGESTION

A summary of all collected HPLC digestion fractions and the corresponding mass spectrometry of peptide fragments are detailed in Table 2-1. After chymotrypsin digestion, 4 peaks were collected from HPLC at times 5.1, 11.1, 16.1 and 24.7 minutes (Figure 2-14). The elution times indicate digested fragments, none of which correspond to the control peptide indicating digestion continued to completion. In fraction B1, fragments were detected at 824.6m/z and 926.9m/z (Figure 2-15). These values correspond to the matrix of the mass spectrometer and are an internal control for the spectrometer. Fraction B2 contained a significant proportion of digested fragment at 830.7m/z which, as seen in the table of predicted values corresponds to Ac-CGGNGEPR, a product of trypsin digestion. Digested fraction B3 detected a high amount of peptide fragment Ac-CGGNGEPRGDTY at 1266.7m/z which was the cleaved peptide fragment of interest. In addition the N-terimal end of this cleavage product, RAY(K(FITC))GG-NH2 was also detected in this fraction at 1019.1m/z. Fraction

B4 showed more matrix components at 873.8m/z and 926.7m/z but also showed more of the Ac-CGGNGEPRGDTY cleaved product at 1266.6m/z. The presence of both Ac-CGGNGEPRGDTY and the corresponding RAY(K(FITC))GG-NH2 was an indication that chymotrypsin digestion did not go entirely to completion, however, we were unable to perform mass spectrometry using a wide-scale so it is possible that further chymotrypsin digestion products such as RAY and FITC may have been present at lower m/z than was performed.

2.4 **DISCUSSION**:

An ideal heart valve replacement still does not exist. Allograft heart valves and vessels are commonly used in surgical repair of congenital defects however; complications of allograft tissue including damage after cryopreservation, size and infection (5) limit the success of these surgeries. More importantly, the devastating immune response against these allograft tissues leads to *in-vivo* rejection of the tissue, unless further intervention is applied. While the cell-mediated arm of immune rejection which directly destroys the graft, is mostly understood, the humoral immune response which has been shown to have more lasting effects by sensitizing the patients to the foreign body and building up antibodies in the host, is less well known. Combined, the cell-mediated response leads to an increased need for reoperation, which in turn results in an increased risk of mortality and morbidity (3). Following reoperation the sensitization of the host due to the humoral immune response can then complicate future transplants.

Decellularization of the allograft valve has been shown to significantly reduce both the humoral and the cellular immune response *in-vitro* and *in-vivo*

(6). However, the loss of cellular components, especially the endothelium renders these tissues more susceptible to thrombosis, as has been seen *in-vivo* (6). The increased thrombogenicity can be attenuated through *in-vitro* endothelialization of the decellularized vascular tissue prior to implantation (11,12).

Unfortunately, there is a paucity of research that can show adequate retention of an *in-vitro* seeded endothelium in a working model. *In-vivo*, endothelial cells have been seen to slough off under the impact of shear stress forces (13). The current challenge is to create a functional endothelial monolayer *in-vitro* that is maintained in a living model. In order to retain the neoendothelium onto decellularized tissue endothelial cells must be covalently bound. RGD peptides are known to be important in facilitating endothelial cell binding (14,15) via cell surface integrin receptors (16). These peptides may covalently bind endothelial cells to the decellularized tissue basement membrane, thereby enhancing cellular retention *in-vivo*. The overall goal of this, and other centers is to ultimately repopulate a decellularized tissue using the recipients' own endothelial cells. This custom tissue could be available shortly after the need is discovered. Most importantly, a decellularized scaffold recellularized with autologous cells may potentially grow, repair and remodel itself similar to a native normal functioning tissue. These tissues could endure for the duration of the patients' life, eliminating the need for any subsequent transplantation.

Here we have clearly demonstrated a novel method to attach an RGD peptide fluorescently labeled with FITC to decellularized ovine tissue. We have shown an increased HUVEC cell migration to the endothelial surface of

decellularized ovine tissue with increased cell honing to an RGD modified

surface. There is also a clear indication of neoendothelium formation after 3 days

of HUVEC incubation again with increased adhesion on an RGD functionalized

interface. The repopulation of decellularized ovine tissue with HUVEC cells was

confirmed by CD31 staining and the even distribution of HUVECs along the

luminal surface of the tissue samples was clearly shown using confocal

microscopy. Following our histology results, 3 days was recognized as the

optimal time for cell seeding *in-vitro*; after 8 days in static conditions, HUVEC

cells showed decreased cellular retention and adhesion. Quantitative analysis of

DNA content at 3 days correlated to increased values on samples modified with

RGD vs. control samples. Importantly, similar results seen in ovine tissue were

reproducible in a human *in-vitro* model of the same conditions. EMCH addition

was not found to be necessary to covalently bind RGD peptide to the

decellularized surface of human tissue, however, these findings were not

statistically significant, as they clearly were in ovine tissue. Similar histological

results were observed between recellularized human and ovine tissue, using the

optimized 3 day time point for *in-vitro* cell seeding on human tissue. Finally,

DNA content was confirmed to increase after RGD modification, similar to ovine

tissue though neither was found to be statistically significant. In an attempt to

possibly elucidate the binding mechanism of the RGD-FITC peptide to the

surface of decellularized tissue in the future, preliminary studies on a viable

enzymatic digestion of the RGD-FITC peptide to effectively remove the FITC

from the peptide chain were conducted and shown to proceed in a predictable

manner with only minimal non-specific activity. This ultimately creates a clear picture in which a method to bind a FITC modified RGD peptide to the surface of decellularized ovine and human tissue is developed, repopulation of these modified surfaces with HUVEC cells that enhance endothelial cell binding compared to controls is shown, an even distribution of positively identified endothelial cells is evident and finally, a possible mechanism to effectively remove the potentially immunogenic FITC label from the peptide once it has been modified to the tissue surface is confirmed *in-vitro*.

We report that decellularized ovine tissue does exhibit some auto fluorescence and so all subsequent fluorescence measurements must correct for this factor. Our findings, which clearly indicate that the EMCH addition is not necessary to bind our RGD-FITC peptide does not agree with the results of Stile et al after whose work this mechanism of addition was modeled (18). Stile et al showed that in the absence of EMCH addition, their peptide of interest (which also contained an end-terminal cysteine group to spontaneously react with the maleimide group in EMCH) could not be detected. In the absence of EMCH both of our negative control groups (UPW and MES buffer alone) significantly bound the RGD-FITC peptide as was clearly shown by an increase in RFU values. The mechanism by which this peptide is spontaneously binding to decellularized tissue is not known. It is important, however, to note that Stile et al attempted to modify poly acrylic acid linear chains whereas we modified decellularized ovine collagen therefore the mechanism of peptide binding to collagen tissue may negate the need for EMCH addition. It is possible that the reactive FITC N-terminus of the

73

peptide is responsible for the covalent binding however, the thiol groups conjugated to the C-terminus of the peptide remains the most likely mechanism of addition. Thiol groups are known to be extremely highly reactive and bind specifically to proteins present in collagen (19). This is seen at a pH range used in our RGD-modification step as well as at room temperature. The reactivity of FITC proceeds at a higher temperature than was used in our experiment. After repetition of this study to show reproducibility all subsequent studies involving RGD-FITC modification did not utilize the EMCH step and decellularized tissue was simply reacted with peptide spontaneously to decrease tissue preparation time.

HUVEC cells showed cell surface and intracellular markers that concur with the literature for functional endothelial cells (20). In addition, our 18 amino acid peptide with the known RGD sequence of interest was seen to effectively bind HUVEC cells when incubated in suspension at 10μM and almost completely at 50μM. This evidence is consistent with literature that also shows this identical peptide sequence to have increased osteoblast cell binding (21). As a result of the increased HUVEC binding at 50μM RGD-FITC all subsequent HUVEC binding studies using RGD modified decellularized tissue were reacted with 50μM RGD-FITC and not 10μM and 50μM was deemed the optimal ligand concentration for binding HUVEC cells.

In accordance to our findings above, the HUVEC binding to RGD decellularized ovine tissue did not include an EMCH addition prior to RGD-FITC addition onto tissue. Interestingly, our results indicate a significant difference in

auto fluorescence between our randomly allocated decellularized ovine tissue disks; this was not seen previously. While it is important to note this difference, however, the auto fluorescence measures were 36.40±9.33 vs. 44.44±9.85 and while 44.44 may be significantly higher than 36.40 the RFU measures jump to 3707±503 when RGD-FITC was added compared to 35.57±10.23. This exponential jump in fluorescence cannot be attributed to the slightly higher fluorescence seen in the basal tissues, thus we can say with confidence that our groups do not show any confounding effects due to differences in auto fluorescence. Histological analysis revealed almost no HUVEC cell binding at $1x10^4$ and $1x10^5$ cells for either RGD or control ovine tissues at 36 hours. This leads us to believe that at these lower cell concentrations there is not enough of an interaction between an adequate number of HUVECs and the endothelial surface to maintain cellular migration through to the fixation process. Accordingly, we did not expect to see any HUVEC binding on $1x10^4$ and $1x10^5$ cell concentration disks after 72 hours since there was no evidence of any cellular migration at 36 hours. This was confirmed by the histology with showed an absence of purple basophilic structures in all 8 of these samples. Compared to $1x10^4$ and $1x10^5$ cells, $1x10^6$ cells showed a significantly higher cell migration to the endothelial surface at 36 hours on both RGD and control samples. This agrees with other studies that have shown endothelial cell migration and adhesion to non-treated surfaces *in-vitro* (22). Importantly, the RGD functionalized endothelial surface appears to increase HUVEC migration through increased cell number and potentially increased cell-surface interactions than our control disks at 3 days post

incubation. We propose that the RGD ligand facilitates a covalent interaction to HUVECs, 'tethering' these cells to the surface and preventing their displacement. This is important because this will increase the number of cells which are capable of laying flat and form a tight confluent endothelial monolayer over time. This postulation was confirmed with our histology slides at 72 hours. Both the RGD and the control samples showed significant endothelialization compared to the $1x10^4$ and $1x10^5$ samples of the same time point. However, as can be seen in the figure, RGD functionalized tissue again appears to show enhanced HUVEC adhesion compared to control. This is important to show that even *in-vitro*, RGD shows more potential for the creation a confluent monolayer than simply adding endothelial cells to untreated collagen surfaces, so studies that have shown minimal retention of endothelium *in-vivo* may benefit from a method that enhances endothelial cell adhesion to the basement membrane of vascular tissue prior to implantation. Interestingly, at 8 days post incubation of HUVEC cells we noted decreased cellular adhesion and confluency. This leads us to believe that 3 days is likely the most optimal period of time for *in-vitro* cell seeding of decellularized tissues under static conditions.

Immunofluorescence staining of our repopulated decellularized ovine tissue confirmed that the endothelial cells seen in the histology are in fact HUVEC in nature, and not remnant native cells from the original tissue. An absence of DAPI staining in the collagen of the ECM clearly indicates a lack of cells, confirming the completeness of decellularization. Ovine tissue autofluorescence was seen with both rhodamine and FITC filters, however

increased FITC fluorescence with RGD modification indicates positive RGD binding which correlates to our fluorometer data. Importantly, the fluorometer will not tell us how the cells are oriented upon the tissue disks, only that there is enough bound peptide to indicate a significant increase in fluorescence compared to controls. Thus, confocal imaging allows us to show that ECs are not all clumped in patches or areas, but rather spread out profusely on the surface, likely falling into crevices and valleys naturally occurent upon the luminal surface topography. Further, this is promising to lend itself to a more confluent monolayer of cells once they are in-situ and able to hone new cells to the luminal surface and proliferate.

Characterization of the RGD-FITC peptide prior to modification onto tissue detected minimal amounts of RGD peptide without the FITC label, indicating that the stability of the FITC peptide is enough to warrant that the fluorometer data used to quantitatively show RGD peptide modification onto decellularized tissue is accurate and not confounded by any significant loss of the FITC peptide from immobilized peptides on the surface of the tissue. In addition, after chymotrypsin digestion there was very little evidence of non-specific cleavage of the peptide after the R group of RGD via trypsin contamination, therefore, we infer that overnight digestion via high purity chymotrypsin is a viable digestion for eliminating the FITC group after modification onto decellularized tissue. Future studies will have to be conducted to confirm the same endothelial cell adhesion to decellularized surfaces after FITC digestion of the peptide.

Due to the current superiority of allograft tissue to any other potential graft alternative we have reproduced the optimal conditions of our ovine repopulation studies in a human *in-vitro* model. We have shown that the results seen in decellularized ovine tissue results in similar repopulation patterns and optimization in human tissue based upon histological analysis and DNA content. While statistical significance was not seen in any of the human studies, likely due to the increased autofluoresence of human decellularized tissue compared to ovine, the trend of the values clearly indicates that ovine tissue is an excellent model to optimize all unknown conditions necessary for tissue engineering of decellularized grafts prior to testing on human tissue so as not to waste any valuable human allografts available for research purposes.

A necessary next step will be to evaluate the functionality of these re-endothelialized surfaces using functional assays of platelet adhesion and eNOS secretion. These may give us an idea as to how this endothelium will behave in a working model.

In addition, the cellular retention of our RGD functionalized decellularized tissue remains to be seen. While some researchers believe that the actual endothelial cell seeding process should also occur in a pulsatile bioreactor (23) we believe that under static conditions cells are more capable of forming a confluent monolayer, and this has been seen in the literature (22). An *in-vitro* monolayer can then be tested for retention using a pulsatile bioreactor specifically designed to mimic physiological conditions such as shear stress, pH, gas exchange and temperature. In this way, our endothelium can be tested for retention as well as

the ability to enhance endothelial cell migration to sites of non-confluency, from our static model, and show repair capabilities.

2.5   CONCLUSIONS

We have described a novel method to attach a FITC labeled RGD containing peptide to decellularized ovine and human tissue. Our results clearly indicate that at a concentration of $1x10^6$ cells/30mm we can achieve an increased re-endothelialization on RGD functionalized decellularized ovine and human tissue compared to non-treated decellularized tissue. This results in increased cell migration at 36 hours and higher cell adhesion and monolayer formation at 3 days post incubation. In addition, we have done preliminary work on a method of RGD-FITC digestion that effectively cleaves the FITC fragment from the RGD containing peptide for future *in-vivo* work. This is an important first step to realizing the goal of an autologous custom transplantable vascular tissue that is capable of growth and repair.
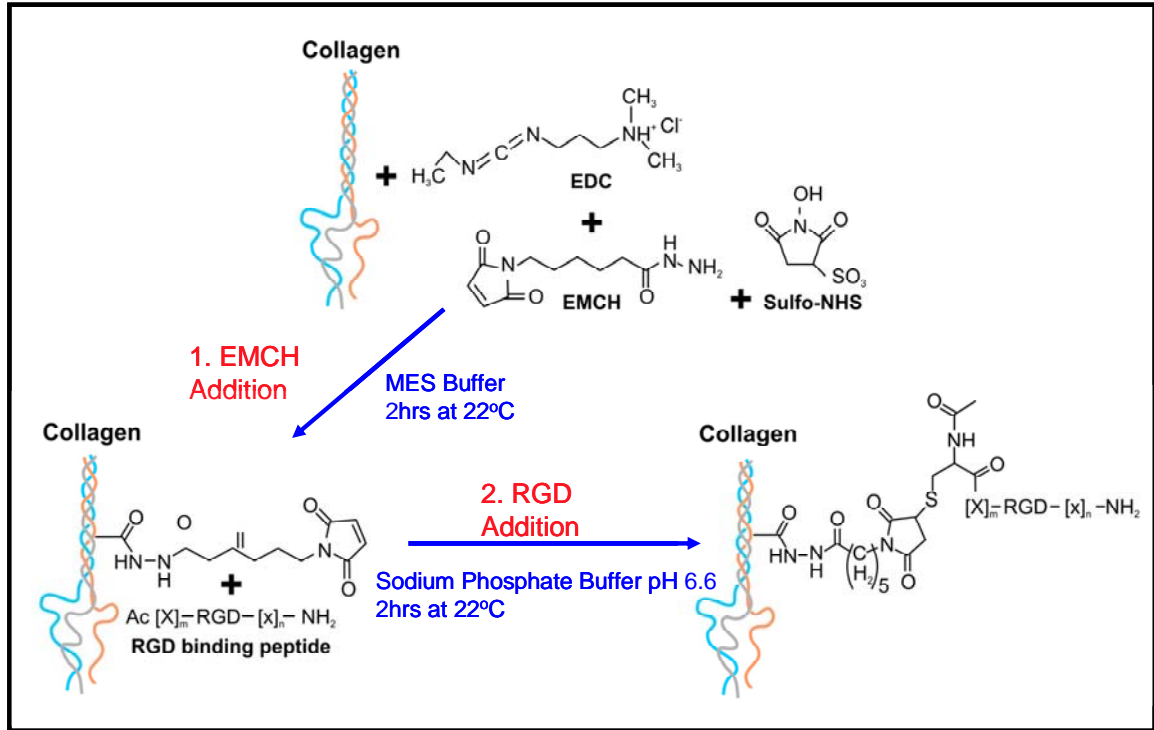
Figure 2-1. Modified 2-Step Method for Functionalization of RGD-FITC Peptide onto Decellularized Tissue Surface

Schematic showing the proposed two step binding mechanism of RGD-FITC to the collagen luminal surface of decellularized tissue. The first step includes the use of reducing agents EDC and sulfo-NHS to create a maleimide ester after EMCH addition. The following step exploits a spontaneous reaction between the highly reactive thiol group on the C-terminus of the RGD-FITC peptide with the covalently bound maleimide ester present on the collagen surface resulting in a covalently bound RGD sequence on our decellularized matrix.

Native vs. Decellularized Sheep Pulmonary Artery
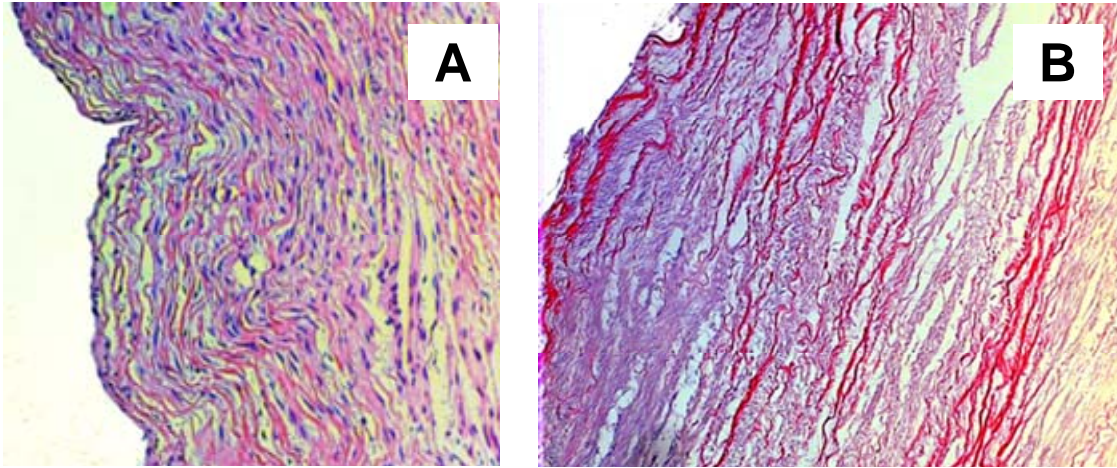
Figure 2-2. Comparison of Native vs. Decellularized Sheep Pulmonary Artery

Representative histology using Haematoxylin and Eosin staining, of native sheep pulmonary artery taken immediately after thawing of cryopreserved tissue (A), and after hypotonic and hypertonic cell lysis decellularization (B). Note the absence of both endothelial cells and interstitial cells within the extracellular matrix.
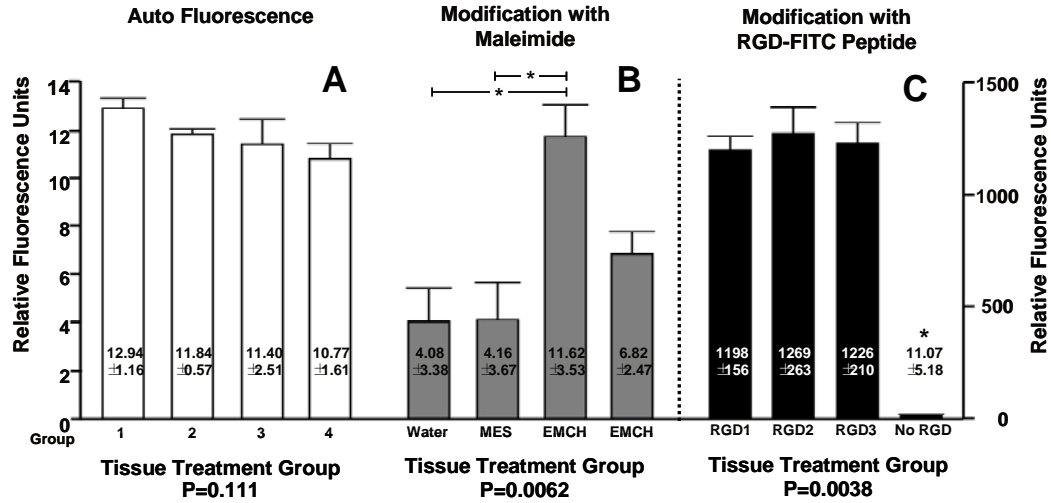
Figure 2-3. RGD Functionalization onto Decellularized Tissue

Decellularized tissue exhibits some auto fluorescence in all 4 randomly allocated groups (A) but EMCH addition only showed significant increase in fluorescence in one of the two groups treated (B). Fluorescence after RGD-FITC addition shows significant increases in fluorescence for both negative control groups for EMCH addition as well as our experimental group but not in our negative control group for RGD (C). Significance is indicated with an asterisk.
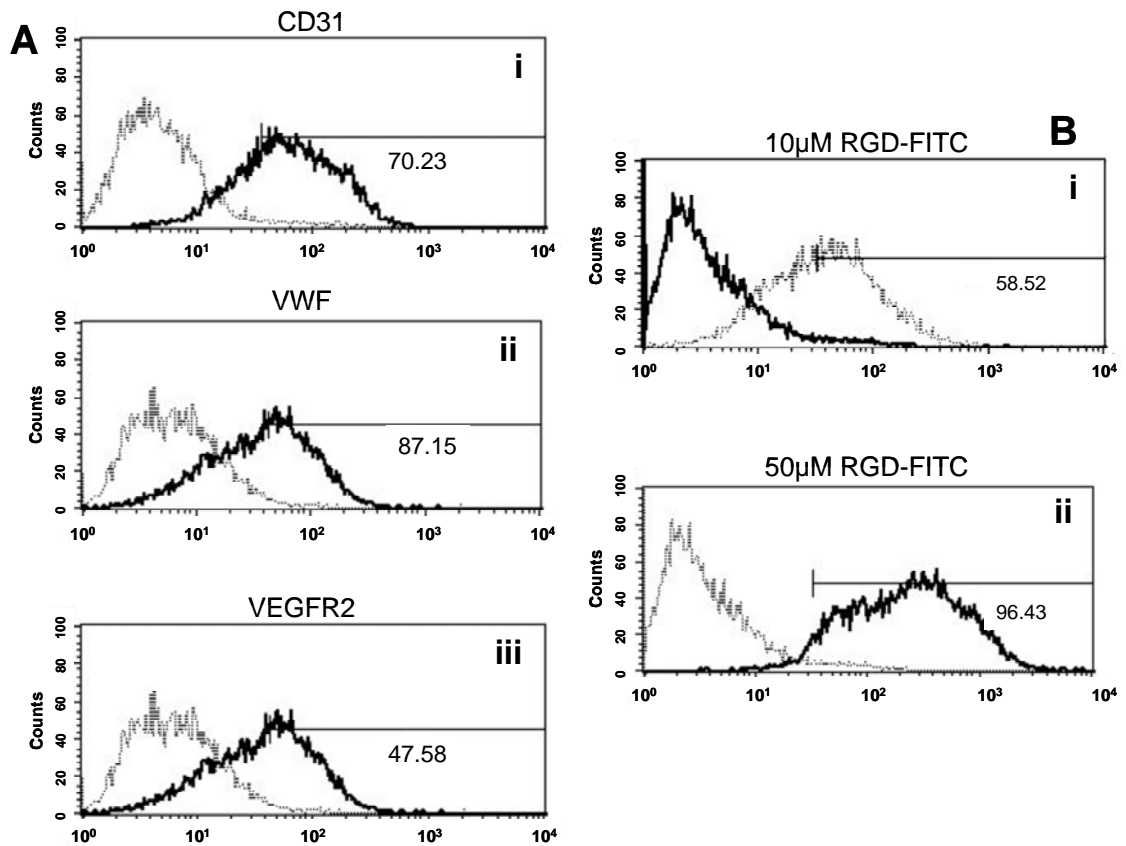
Figure 2-4. HUVEC Characterization and RGD Binding Affinity

Cells were stained positive for CD31(i) and VWF (ii) and most were stained positive for VEGFR2 (iii) (A). HUVEC-RGD binding showing both 10μM (i) and 50μM (ii) (B).
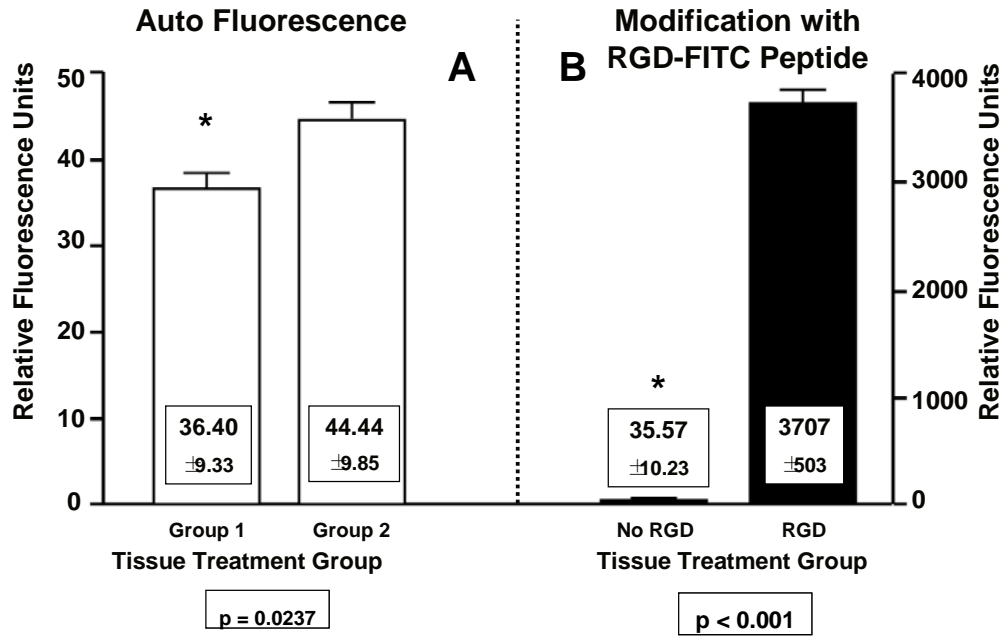
Figure 2-5. RGD Functionalization onto Decellularized Tissue: Modified Protocol

Decellularized tissue auto fluorescence for both randomly allocated groups (A) and fluorescence after RGD-FITC addition at 50µM (B). Note: the scale for 4A is 1-50 RFUs while the scale for 4B is 1-4000 RFUs.

A
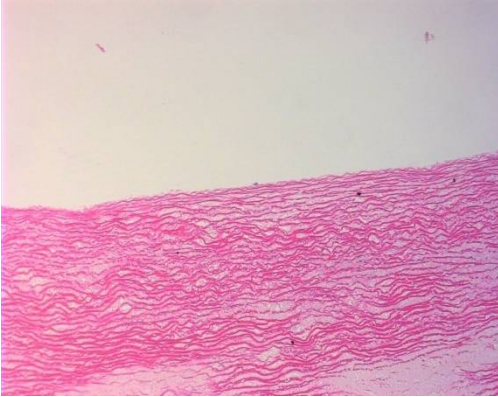
36hr 1x10^4 HUVECs
No RGD
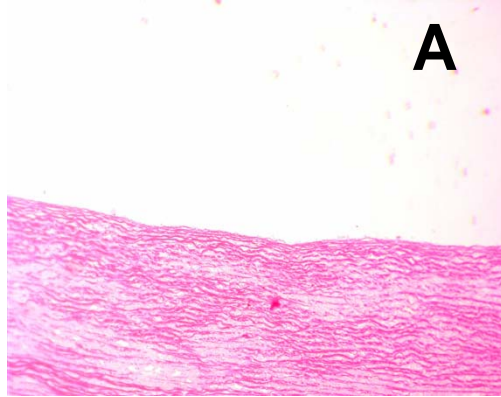
36hr 1x10^4 HUVECs
RGD

36hr 1x10^5 HUVECs
No RGD
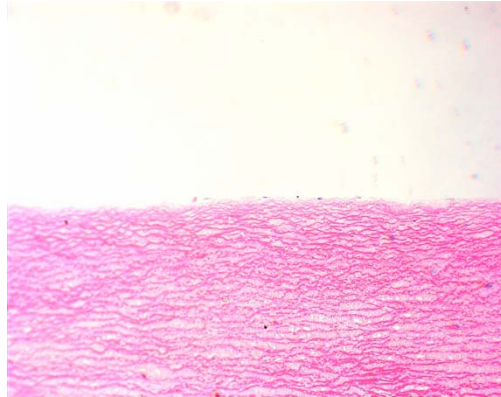
36hr 1x10^5 HUVECs
RGD
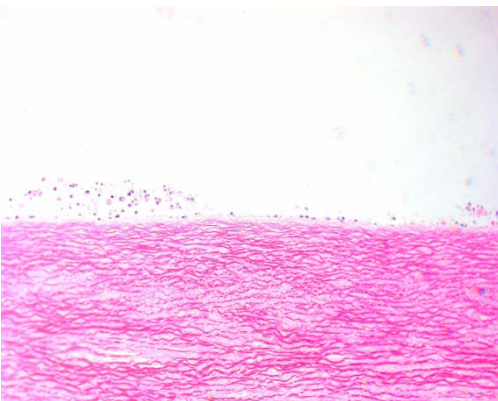
36hr 1x10^6 HUVECs
No RGD
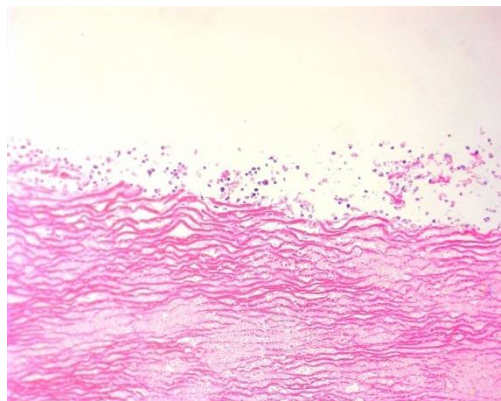
36hr 1x10^6 HUVECs
RGD

B
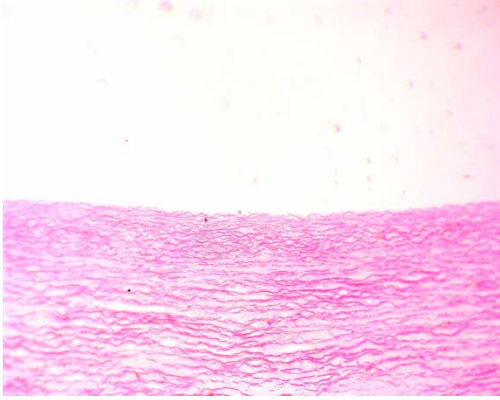
D3 1x10^4 HUVECs
No RGD
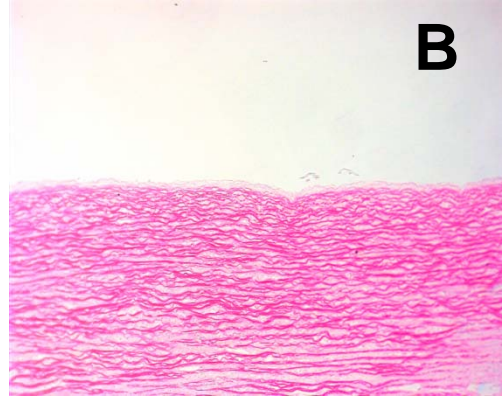
D3 1x10^4 HUVECs
RGD
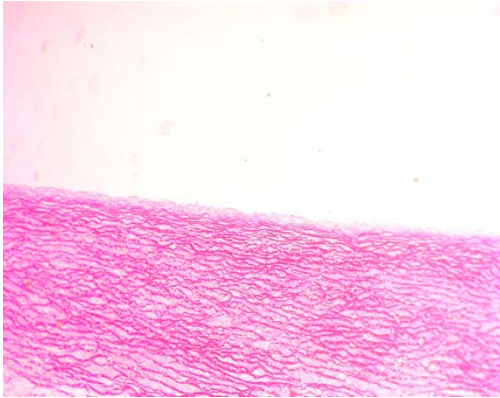
D3 1x10^5 HUVECs
No RGD
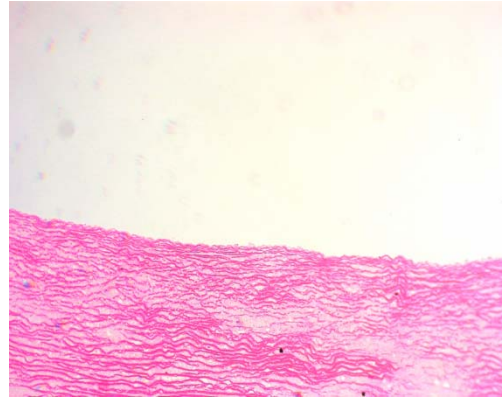
D3 1x10^5 HUVECs
RGD
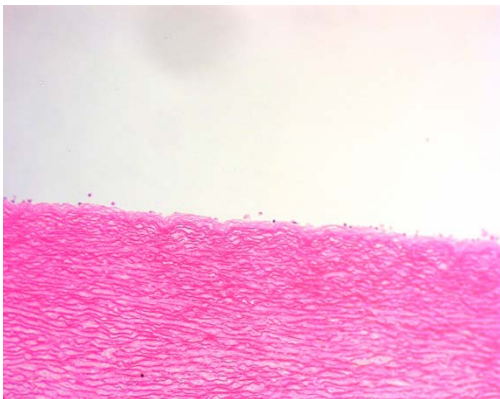
D3 1x10^6 HUVECs
No RGD
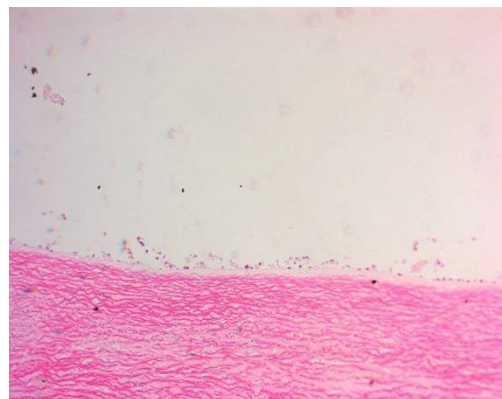
D3 1x10^6 HUVECs
RGD
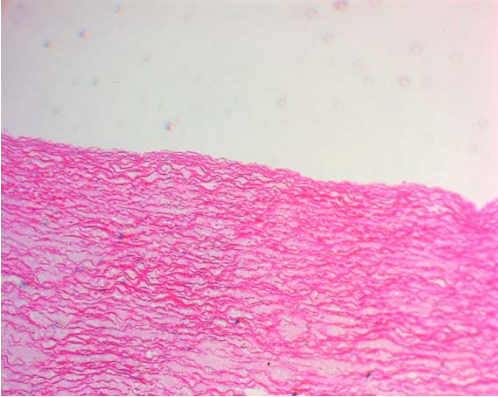
D8 1x10^4 HUVECs
No RGD
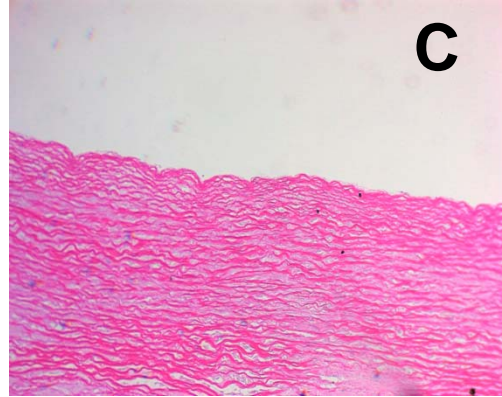
D8 1x10^4 HUVECs
RGD
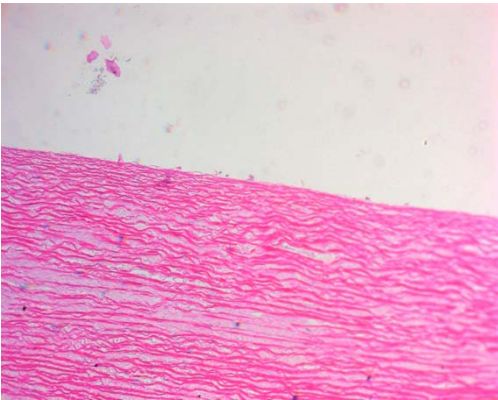
D8 1x10^5 HUVECs
No RGD
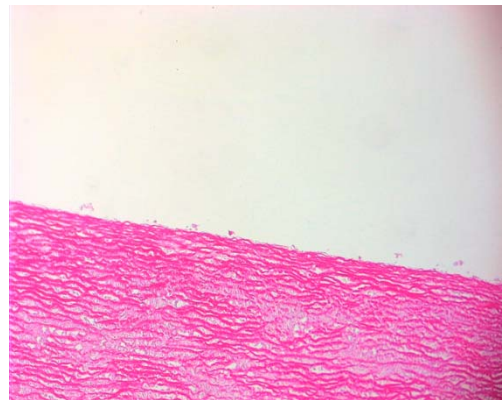
D8 1x10^5 HUVECs
RGD
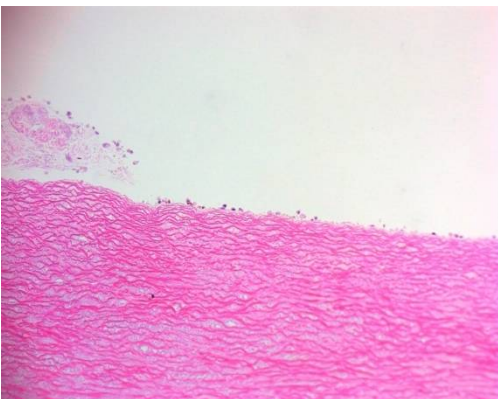
D8 1x10^6 HUVECs
No RGD
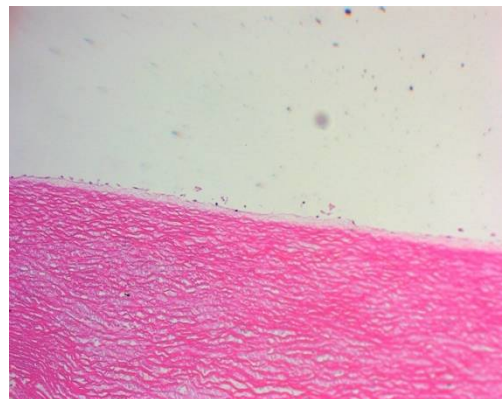
D8 1x10^6 HUVECs
RGD

Figure 2-6. HUVEC Binding to RGD Functionalized Decellularized Ovine Tissue at 36 Hours, Day 3 and Day 8

Representative histology using Haematoxylin and Eosin staining of samples at cell concentrations of $1x10^4$, $1x10^5$ and $1x10^6$ cells per disk for control and RGD modified decellularized tissue after 36 hours (A), 72 hours (B) and 8 days (C) after HUVEC cell incubation (100x magnification).
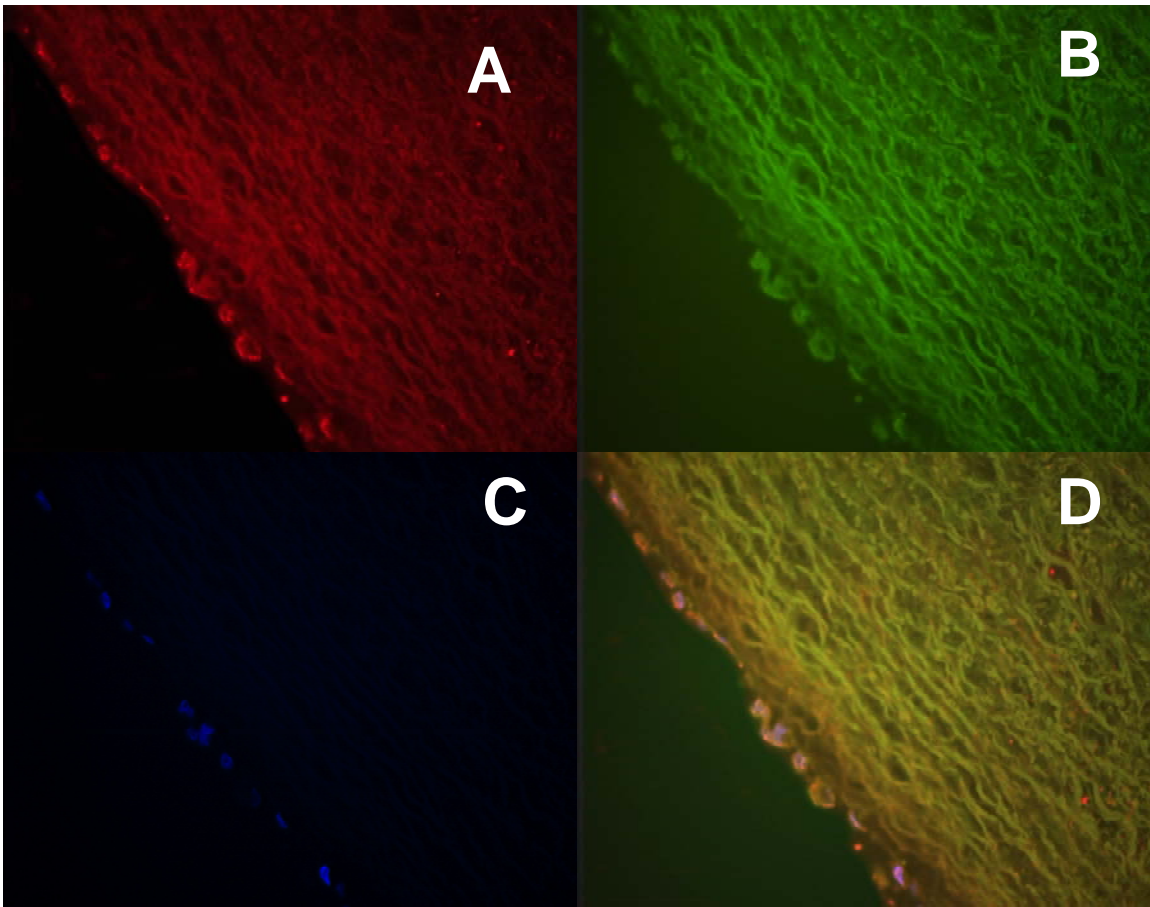
Figure 2-7. Fluorescence Imaging of RGD-Modified Decellularized Ovine Tissue After 3 Days of HUVEC Cell Incubation

Anti-CD31 staining to positively identify HUVEC cells was performed. Rhodamine labeled HUVEC cells are visible in A. FITC fluorescence seen in B is indicative of a higher than basal level of fluorescence due to modification with the FITC labeled peptide. DAPI staining (C) shows a layer of endothelium present on the luminal surface of decellularized tissue with no nucleic acid staining in the tissue confirming decellularization. An overlay of all three fluorescent images is shown in D (200x magnification).
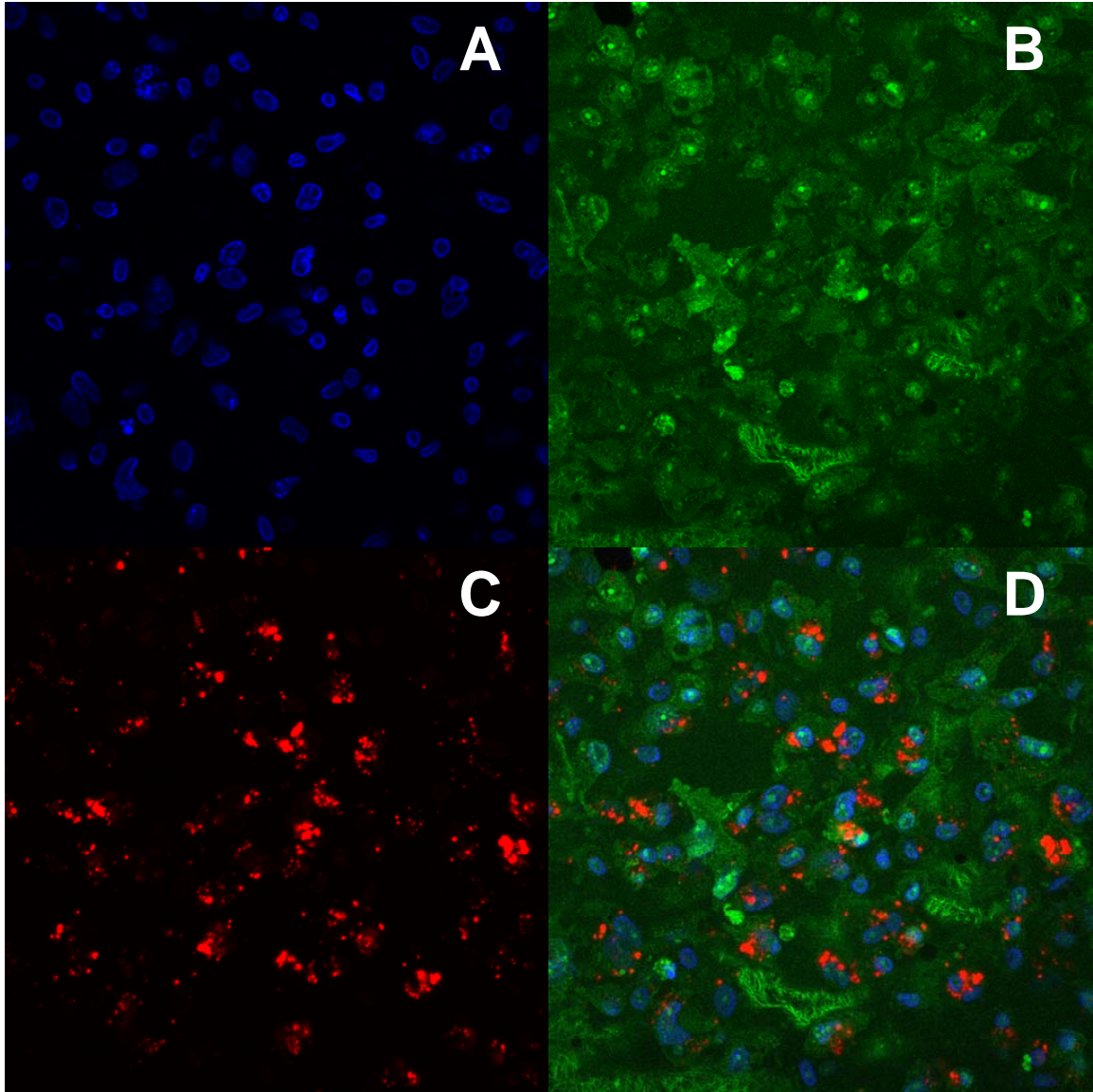
Figure 2-8. Confocal Imaging of Tissue Sample Luminal Surface

Confocal images taken after 3 days of HUVEC cell incubation on RGD
modified tissue samples using DAPI (A) for nuclei staining, FITC (B) detection
of the RGD-peptide and Q-Dot Cell Tracker Red (C) dye for HUVEC cell
identification. A compound overlay of all images is seen in D. Note: distribution
of DAPI and Q-Dot dye indicates evenly dispersed cell adhesion.

DNA Quantification Assay
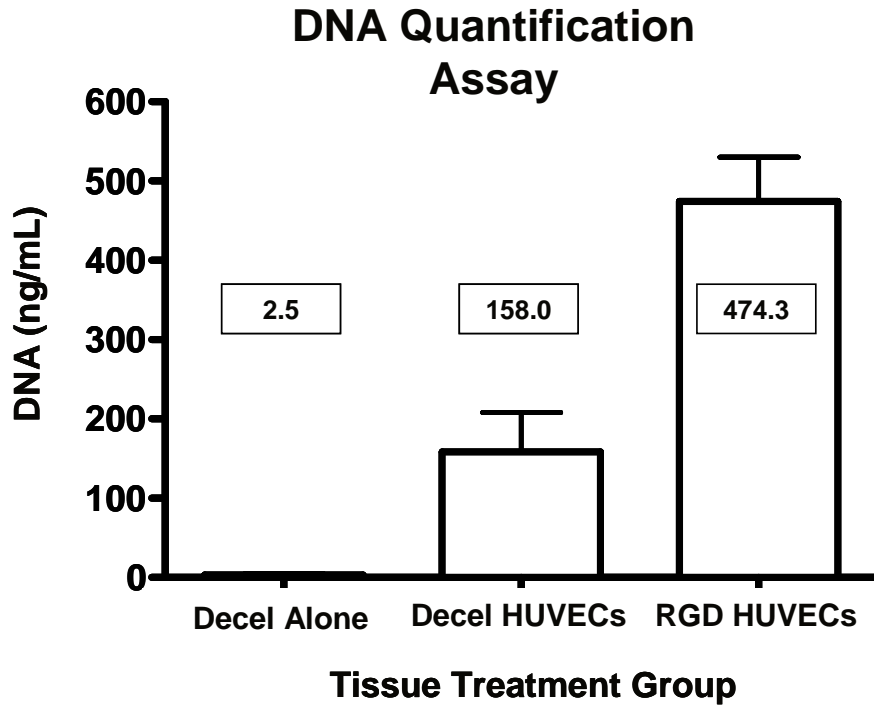
Figure 2-9. Quantitative Assessment of DNA Content of Day 3 Samples of Repopulated Decellularized Ovine Tissue

Comparison of the DNA content measured as ng/mL of sample for decellularized disks alone, decellularized disks incubated with $1x10^6$ HUVECs and RGD-modified decellularized disks incubated with $1x10^6$ HUVECs.
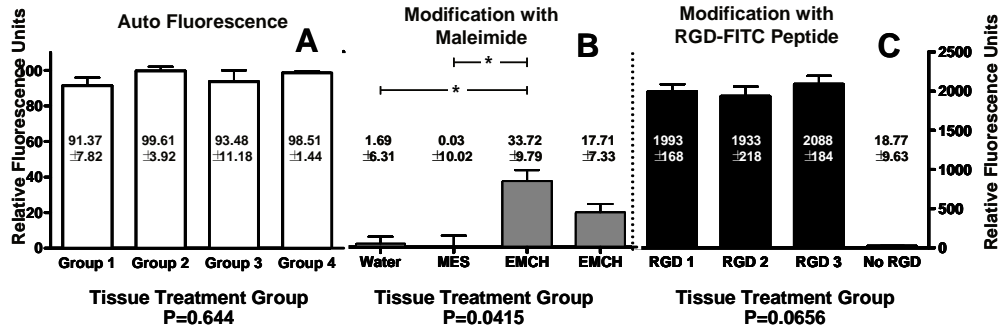
Figure 2-10. RGD Functionalization onto Decellularized Human Tissue

Decellularized tissue exhibits some auto fluorescence in all 4 randomly allocated groups (A) but EMCH addition only showed significant increase in fluorescence in one of the two groups treated (B). Fluorescence after RGD-FITC addition shows increases in fluorescence for both negative control groups for EMCH addition as well as our experimental group but not in our negative control group for RGD (C). Significance is indicated with an asterisk.
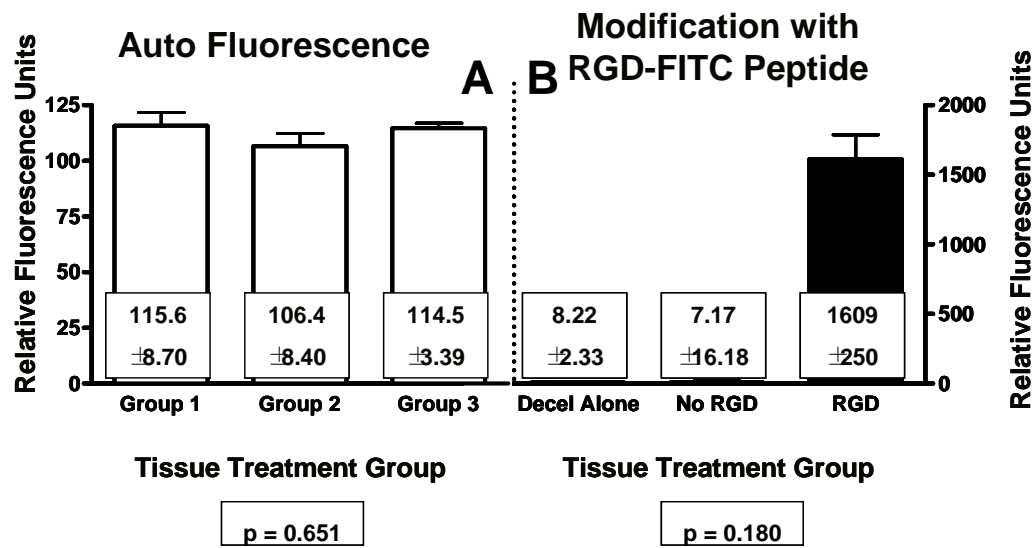
Figure 2-11. RGD Functionalization onto Decellularized Human Tissue:

Modified Protocol

Decellularized tissue auto fluorescence for three randomly allocated

groups (A): decellularized tissue alone (Group 1), decellularized tissue incubated

with $1x10^6$ HUVECs (Group 2) and RGD modified decellularized tissue

incubated with $1x10^6$ HUVECs (B). Note: the scale for 4A is 1-125 RFUs while

the scale for 4B is 1-2000 RFUs.
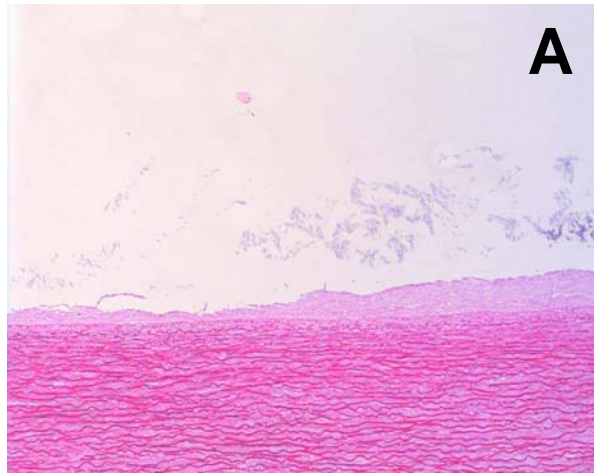
Decellularized Tissue
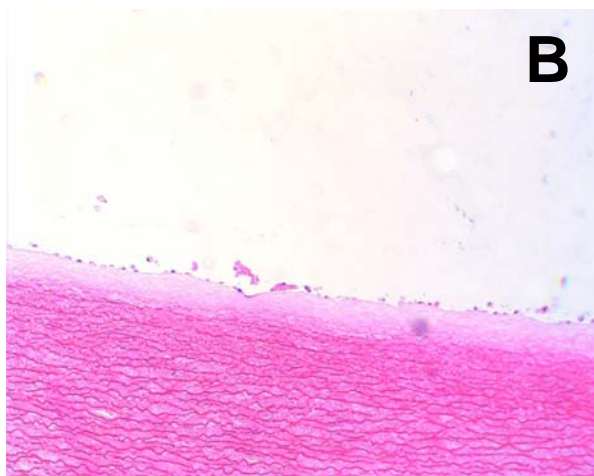
Decellualrized Tissue With HUVECs
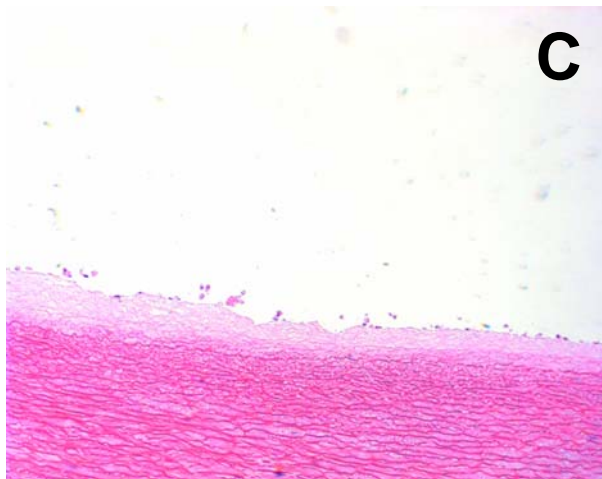
RGD Modified Decellularized Tissue With HUVECs

Figure 2-12. HUVEC Binding to RGD Functionalized Decellularized Human Tissue at Day 3

Representative histology using Haematoxylin and Eosin staining of samples at cell concentrations of $1x10^6$ cells per disk for decellularized tissue alone (A), HUVECs incubated with decellularized tissue alone (B) and HUVECs incubated with RGD modified decellularized tissue (C) after 3 days (100x magnification).

DNA Quantification Assay
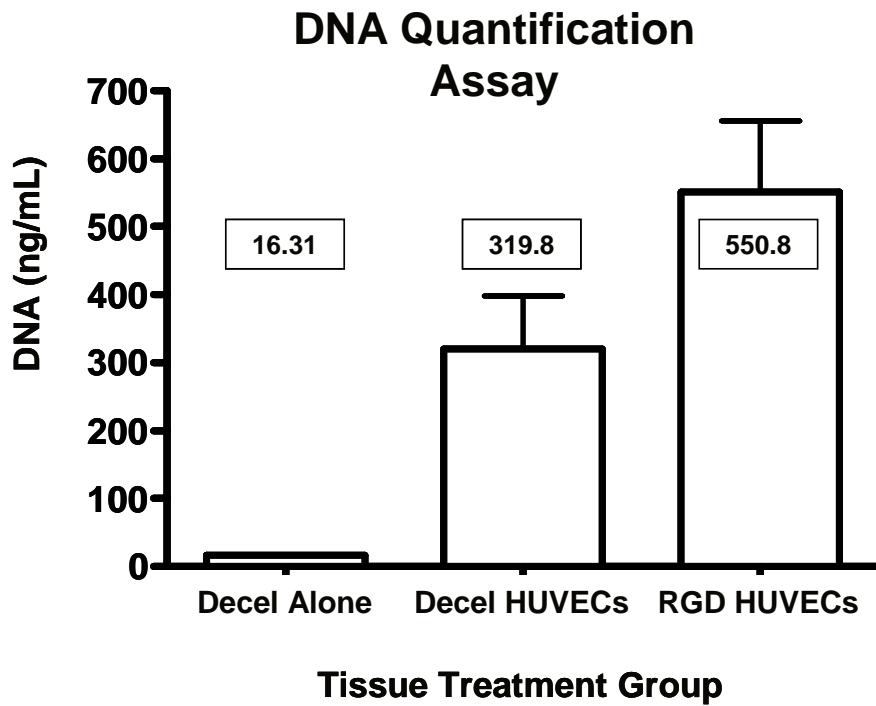
Figure 2-13. Quantitative Assessment of DNA Content of Day 3 Samples of Repopulated Decellularized Human Tissue

Comparison of the DNA content measured as ng/mL of sample for decellularized disks alone, decellularized disks incubated with $1x10^6$ HUVECs and RGD-modified decellularized disks incubated with $1x10^6$ HUVECs.

Predicted Species	Molecular Weight g/mol	Detected	Fraction
Ac-CGGNGEPRGDTYRA(K(FITC))GG-NH2	2287.9	2290.0	A1
Ac-CGGNGEPRGDTYRAY	1657.7		
Ac-CGGNGEPRGDTY	1267.3	1266.7	B3 B4
RAY(K(FITC))GG-NH2	1020.6	1019.1	B3
Ac-CGGNGEPR	830.9	830.7	B2

Table 2-1. Predicted Fragments of RGD-FITC Peptide after Chymotrypsin Digestion

Predicted fragments are listed and the corresponding detected fragments are shown. The fractions from which the digested fragments were collected are also shown. Predicted data is from a simulated cutter proteolysis program (Stile et al, 2005).
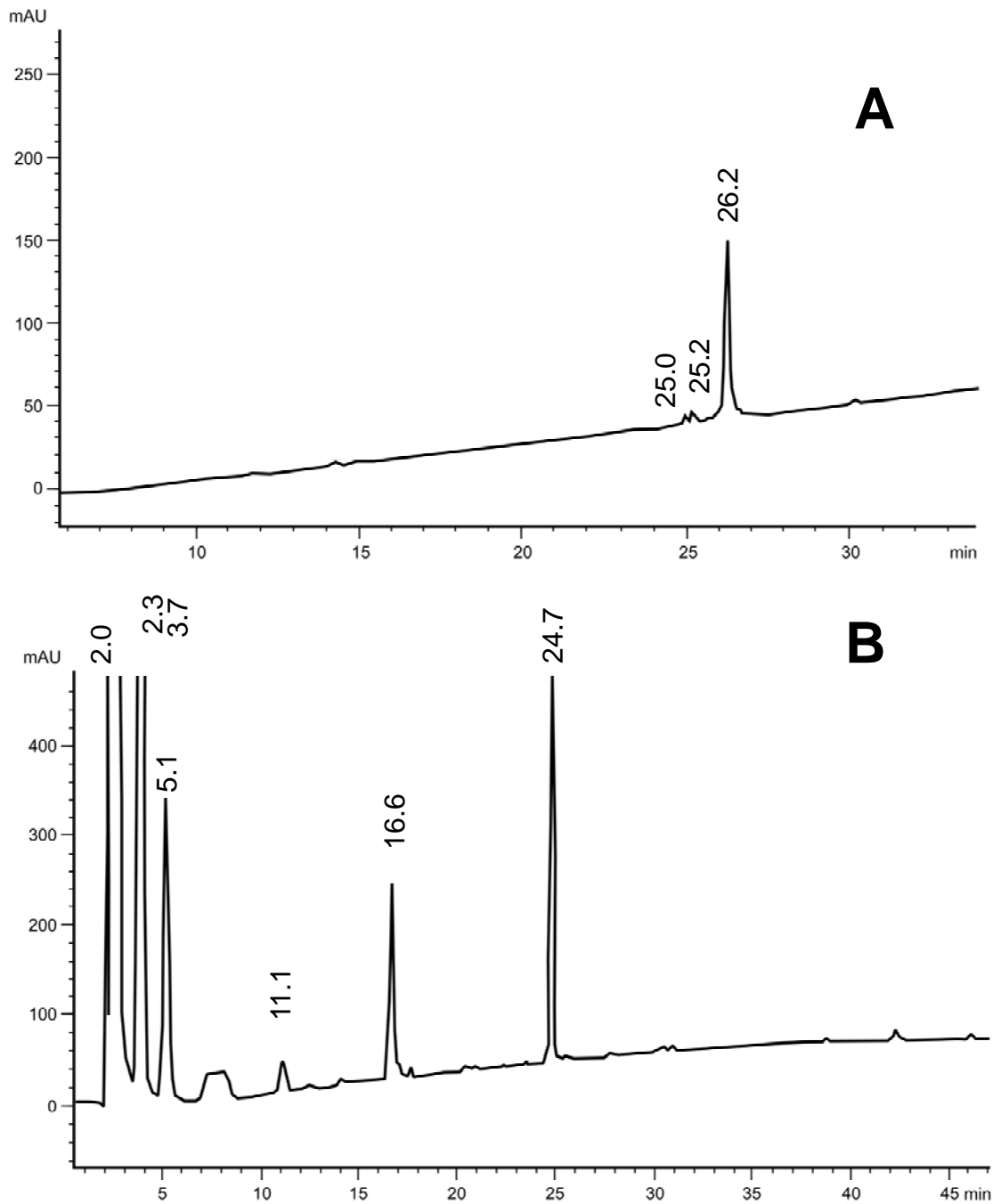
Figure 2-14. HPLC Traces of Undigested and Digested RGD-FITC Peptide

Elutions A1 and B1, B2, B3 and B4 were collected and further analyzed

using mass spectrometry. Note: digested fraction eluted out at earlier time points.
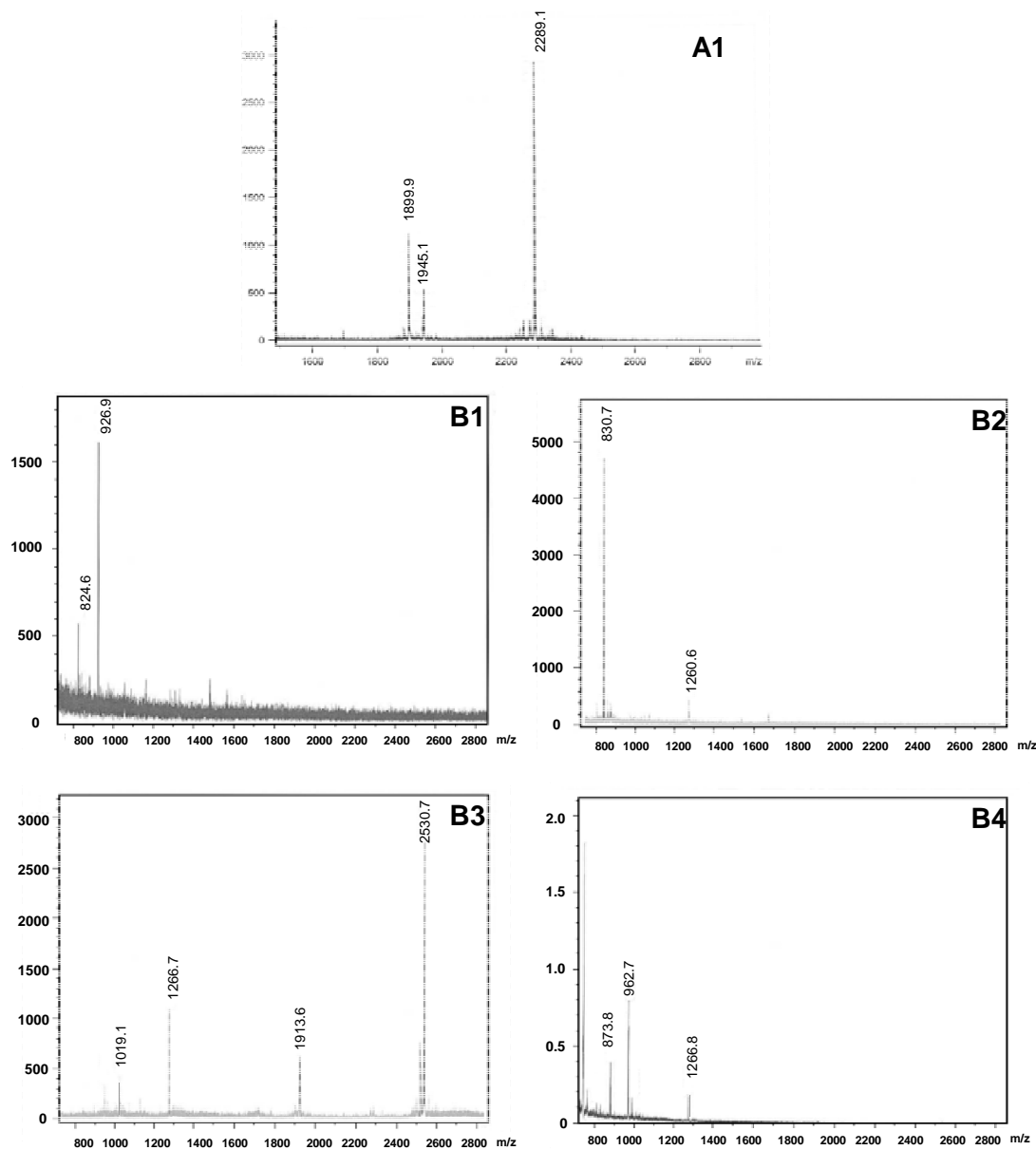
Figure 2-15. Mass Spectrometry Data of RGD Characteriaztion and

Digestion with Chymotrypsin From Collected HPLC Fractions

The mass spectrometry of RGD-FITC control (A1 fraction of HPLC) and

chymotrypsin digestion products (B1, B2, B3 and B4 fractions of HPLC) are

shown. Recognizable peptide fragments are shown and highlighted in Table 1.

2.6   REFERENCES

1. Miatton M, De Wolf D, Francois K, Thiery E, Vingerhoets G. Neurocognitive consequences of surgically corrected congenital heart defects: A review. Neuropsychol Rev. 2006 Jun;16(2):65-85.

2. Hammermeister K, Sethi GK, Henderson WG, Grover FL, Oprian C, Rahimtoola SH. Outcomes 15 years after valve replacement with a mechanical versus a bioprosthetic valve: Final report of the veterans affairs randomized trial. Journal of the American College of Cardiology,. 2000 10;36(4):1152-8.

3. Ascenzi JA, Kane PL. Update on complications of pediatric cardiac surgery. Crit Care Nurs Clin North Am. 2007 Dec;19(4):361,9, v.

4. Quader MA, Rosenthal GL, Qureshi AM, Mee RB, Mumtaz MA, Joshi R, et al. Aortic valve repair for congenital abnormalities of the aortic valve. Heart Lung Circ. 2006 Aug;15(4):248-55.

5. Shaddy RE, Hawkins JA. Immunology and failure of valved allografts in children. Ann Thorac Surg. 2002 Oct;74(4):1271-5.

6. Meyer SR, Nagendran J, Desai LS, Rayat GR, Churchill TA, Anderson CC, et al. Decellularization reduces the immune response to aortic valve allografts in the rat. J Thorac Cardiovasc Surg. 2005 Aug;130(2):469-76.

7. Hogan PG, O'Brien MF. Improving the allograft valve: Does the immune response matter? J Thorac Cardiovasc Surg. 2003 Nov [cited 3/31/2008];126(5):1251-3.

8. Baskett RJ, Ross DB, Nanton MA, Murphy DA. Factors in the early failure of cryopreserved homograft pulmonary valves in children: Preserved immunogenicity? J Thorac Cardiovasc Surg. 1996 Nov;112(5):1170,8; discussion 1178-9.

9. Dignan R, O'Brien M, Hogan P, Thornton A, Fowler K, Byrne D, et al. Aortic valve allograft structural deterioration is associated with a subset of antibodies to human leukocyte antigens. J Heart Valve Dis. 2003 May;12(3):382,90; discussion 390-1.

10. Rose EA, Pepino P, Barr ML, Smith CR, Ratner AJ, Ho E, et al. Relation of HLA antibodies and graft atherosclerosis in human cardiac allograft recipients. J Heart Lung Transplant. 1992 May-Jun;11(3 Pt 2):S120-3.

11. Kaushal S, Amiel GE, Guleserian KJ, Shapira OM, Perry T, Sutherland FW, et al. Functional small-diameter neovessels created using endothelial progenitor cells expanded ex vivo. Nat Med. 2001 Sep;7(9):1035-40.

12. Sutherland FW, Perry TE, Yu Y, Sherwood MC, Rabkin E, Masuda Y, et al. From stem cells to viable autologous semilunar heart valve. Circulation. 2005 May 31;111(21):2783-91.

13. Meinhart JG, Schense JC, Schima H, Gorlitzer M, Hubbell JA, Deutsch M, et al. Enhanced endothelial cell retention on shear-stressed synthetic vascular grafts precoated with RGD-cross-linked fibrin. Tissue Eng. 2005 May-Jun;11(5-6):887-95.

14. Ruoslahti E. Fibronectin and its receptors. Annu Rev Biochem. 1988;57:375-413.

15. Pierschbacher MD, Ruoslahti E. Variants of the cell recognition site of fibronectin that retain attachment-promoting activity. Proc Natl Acad Sci U S A. 1984 Oct;81(19):5985-8.

16. Hynes RO. Integrins: A family of cell surface receptors. Cell. 1987 Feb 27;48(4):549-54.

17. Lehr EJ, Hermary S, McKay RT, Webb DN, Abazari A, McGann LE, et al. NMR assessment of me(2)SO in decellularized cryopreserved aortic valve conduits. J Surg Res. 2007 Jul;141(1):60-7

18. Stile RA, Shull KR, Healy KE. Axisymmetric adhesion test to examine the interfacial interactions between biologically-modified networks and models of the extracellular matrix. Langmuir. 2003;19(5):1853-60.

19. Reulen SW, Brusselaars WW, Langereis S, Mulder WJ, Breurken M, Merkx M. Protein-liposome conjugates using cysteine-lipids and native chemical ligation. Bioconjug Chem. 2007 Mar-Apr;18(2):590-6.

20. Ingram DA, Mead LE, Tanaka H, Meade V, Fenoglio A, Mortell K, et al. Identification of a novel hierarchy of endothelial progenitor cells using human peripheral and umbilical cord blood. Blood. 2004 Nov 1;104(9):2752-60.

21. Kim S, Chung EH, Gilbert M, Healy KE. Synthetic MMP-13 degradable ECMs based on poly(N-isopropylacrylamide-co-acrylic acid) semi-interpenetrating polymer networks. I. degradation and cell migration. J Biomed Mater Res A. 2005 Oct 1;75(1):73-88.

22. Lichtenberg A, Tudorache I, Cebotari S, Suprunov M, Tudorache G, Goerler H, et al. Preclinical testing of tissue-engineered heart valves re-endothelialized under simulated physiological conditions. Circulation. 2006 Jul 4 [cited 3/31/2008];114(1 Suppl):I559-65.

23. Hoerstrup SP, Sodian R, Sperling JS, Vacanti JP, Mayer JE,Jr. New pulsatile bioreactor for *in-vitro* formation of tissue engineered heart valves. Tissue Eng. 2000 Feb;6(1):75-9.

3 GENERAL DISCUSSION AND CONCLUSIONS

3.1 DISCUSSION:

Generally, congenital cardiac disease encompasses many fields including cardiology, palliative care, pharmacology and surgery. Those patients undergoing surgical repair for congenital defects often require reconstruction of major blood vessels, and often require valve replacements. Associated with these allograft tissues is a well documented immune response (1,2). This cell mediated immune response against transplanted tissues results in damage to the tissues, rendering them useless for long-term benefit *in-vivo* (3). This further complicates matters as there has been a recognized humoral immune response to allograft tissue that sensitizes these patients receiving donor tissue (4). Future transplantation in patients who have a buildup of PRA antibodies against allograft tissue results in accelerated rejection if these tissues. As a result, there is an increasing need for an ideal valve replacement. Despite the advancements made in congenital surgery, an ideal heart valve replacement still does not exist. Neither synthetic nor xenogeneic valves are ideal. Both increase chances of infection (5). Synthetic valves calcify quickly (6) and xenogeneic valves lose durability (7). In addition, xenogeneic tissues contain antigens recognized by the host immune system leading to rapid cell mediated rejection of these tissues (8). While these antigens can be masked or removed, zoonotic disease transmission is also a large concern among proponents of allograft tissue (9). Depsite the promises afforded by using xenogeneic tissues for transplantation purposes, current limitations in this field focus future studies

104

on the use of allograft tissue. Allograft (frozen human) heart valves and vessels are commonly used in surgical repair due to their superior handling capabilities and excellent hemodynamics (10). The cryopreservation methods of frozen allograft tissue have historically aimed to preserve the cellular components of the tissues in order to promote increased native functionality *in-vivo*. However, decellularization of the allograft valve has been shown to attenuate both the humoral and the cellular immune response *in-vitro* and *in-vivo* of cryopreserved allograft tissue (11). This lends itself to the idea that cryopreservation methods should not focus upon cellular retention. Instead, developing methods to cryopreserved decellularized tissue for use as scaffolds in tissue engineering may be more practical. Decellularized tissue has been shown to preserve its ECM durability after cryopreservation and there is minimal amounts of residual DMSO present that could complicate any future manipulations with these tissues (12). However, although decellularized valves possess favorable immunogenic characteristics, and can be cryopreserved for long time storage these valves are highly thrombogenic *in-vivo* due to the removal of the endothelial lining present in native tissues (11). This limitation facilitates the necessity of tissue engineering for the repopulation of decellularized scaffolds. Both valvular endothelial cells and valvular interstitial cells are necessary for native valve function, repair and remodeling (13). In the decellularization process, both these important cell types are osmotically lysed to reduce the immunogenicity of these tissues. Repopulation of endothelial and interstitial cells can recover the lost functionality of these cells on the performance of these tissues *in-vivo* (14). Most exciting is the concept of

105

repopulating cryopreserved decellularized scaffolds with cells harvested from the recipient. This could result in a non-immunogenic tissue scaffold with biomechanical strength and handling capabilities equal to native tissues (15) but with autologous cells that will aid in tissue repair and, most importantly in the pediatric population of interest, in the growth of these tissues with the child. Unfortunately, advancements in tissue engineering and biological scaffold repopulation have not adequately shown a long term benefit *in-vivo*. Promising studies have shown *in-vivo* cell migration of endothelial cells to the luminal surface of transplanted decellularized scaffolds (16), however, this migration is minimal and not enough to result in a confluent blood-barrier to prevent thrombogenesis (17). *In-vitro* cell seeding has shown improved clinical outcomes with increased cell migration *in-vivo* after transplantation (14), however, a significant number of endothelial cells seeded *in-vitro* are lost under shear stress and physiological pulse flow, reducing the benefit of *in-vitro* cell seeding (18). Thus, cell seeding shows benefit to reducing the thrombogenicity of decellularized scaffolds *in-vivo* but a method to enhance endothelial cell adhesion to the basement surface is required to maximize *in-vivo* endothelial cell migration and subsequent confluency of the neo-endothelium in these patients.

In Chapter II we have described a method to attach a FITC labeled RGD containing peptide to decellularized ovine and human tissue which has not been shown before. Our results clearly indicate that at a concentration of 1×10^6 cells/30mm we can achieve an increased re-endothelialization on RGD functionalized decellularized ovine and human tissue compared to non-treated

decellularized tissue. This results in cell adhesion and monolayer formation at 3 days post cellular incubation. In addition, we have done preliminary work on a method of RGD-FITC digestion that effectively cleaves the FITC fragment from the RGD containing peptide for future *in-vivo* work.

The most important finding in this body of research is the increased endothelialization seen *in-vitro* using an RGD endothelial cell adhesion ligand to enhance decellularized scaffold repopulation. While the mechanism for the binding of RGD peptide to our decellularized surface was predicted to require the enzymatic addition of a maleimide ester (19), our results clearly indicate that this extra step is not necessary. An important question that is raised is whether the non-specific binding of our RGD-FITC peptide of interest is due to orientation via the FITC group or the highly reactive thiol group present in the C-terimnus cysteine amino acid. Due to time constraints, no control studies were conducted to elucidate this binding mechanism, however, the higher reactivity of thiol groups to protein structures (20) coupled with the temperature and pH of our reaction scheme would point in the direction of thiol site binding to the collagen fibres present in our decellularized scaffolds (ref). In addition, the FITC group was bound onto our 18AA peptide sequence of interest in order to facilitate quantitative fluorescence measurements of peptide addition to our scaffold surface. Thus, the importance of the FITC label to our experiment is only in the first step. To this end, we conducted further studies to distinguish a method to effectively remove this FITC label once modification of our 18AA peptide onto our scaffold was complete. We have shown a specific chymotrypsin digestion

which cleaves our Ac-CGGNGEPRGDTYRAY(K(FITC))GG-NH2 peptide after the first typrosine (Y) amino acid results in the RGD sequence of interest in one fragment and the FITC group in the other. Thus, future *in-vitro* studies can utilize this digestion after RGD-FITC modification onto tissue scaffolds to see if chymotrypsin digestion results in decreased fluorescence of our modified tissue scaffolds. It will also be important to show that cleaved RGD peptide is still capable of enhanced HUVEC binding to the decellularized surface.

The enhanced HUVEC adhesion to RGD functionalized decellularized surfaces is promising for future *in-vitro* and *in-vivo* studies. While some groups have shown re-endothelialization using a pulse duplicator *in-vitro* (21), we have seen the benefit of cell incubation under static conditions. We have shown only 30% of the $1x10^6$ cells originally placed for seeding to have adhered to our surface. In addition, we used a commercially based cell source that is theoretically more robust than cells isolated and characterized form the circulation so it stands to reason that EC progenitors garnered from UCB or another source will be even less likely to adhere to the tissue surfaces in conditions of stress or shear force or pulsatile flow. Therefore, due to the nature of endothelial cell adhesion and the time taken to hone to the site of adhesion, it seems likely that initial static repopulation will be more beneficial to cell retention *in-vivo* than cells seeded using a bioreactor. We propose static *in-vitro* seeding for a minimum of 3 days and a maximum of 5 days prior to implantation or testing in a bioreactor. This allows the ECs to adhere, lay flat and begin secreting chemokines etc for proliferation prior to assault by the physiological conditions of the body or a

simulator. The main concept behind cell seeding using a bioreactor is that circulating cells will migrate to the luminal surface through the use of chemoattractants and ligand-integrin interactions (22). Decellularized tissue shows only minimal retention of native fibronectin on the luminal surface (23). Thus, while some groups believe that precoating of decellularized scaffolds with FN may enhance cell seeding, there is evidence to indicate that FN requires a very specific orientation to the surface in order to facilitate covalent interactions between the important EC binding sites RGD and SSHRN (24,25). Coating of FN onto the surface cannot account for the correct orientation of these binding sites and as such could undermine EC adhesion or impact EC function once on the surface. Thus, even in a bioreactor, precoating with FN may not facilitate migration of ECs to the surface. Instead, coating with RGD sequence may help initiate FN formation and assembly (26). RGD is known to be the initator sequence for FN matrix assembly and secretion from adhesive cells. Thus, if the RGD sequence is modified to the surface and bound to ECs this may facilitate neo FN formation that would contain the correct orientation of FN necessary to promote activation and proliferation of ECs to form a confluent monolayer. This also highlights the necessity of ECs to the function of these tissues. While ECs primarily function as a blood-barrier to prevent thrombogenesis, they also help maintain tissue integrity and serve as repair mediators and in FN assembly (27). Thus, the benefit of seeding decellularized scaffolds with ECs rather than simply coating with another hydrophilic substance to prevent interaction of platelets with

collagen surface is not conducive to the ultimate goal of a fully functional valve substitute.

This body of research has been able to show reproducibility of our optimized studies using ovine tissue into a decellularized human scaffold. As noted in Chapter II, we noted an increased human tissue autofluorescence compared to ovine tissue. Considering the major body of this research has relied upon fluorescence tests to quantitatively assess RGD peptide binding and DNA quantification, it may seem necessary to alter the methodology on human tissue or increase the concentration of RGD-FITC in order to gain a statistically significant increase in fluorescence. However, the optimal binding concentration for HUVEC cells remains 50µM so increasing the peptide concentration to increase fluorescence after RGD modification is not appropriate. The RFU values after RGD modification to human tissue still highlight a positive shift in fluorescence indicating adherence of our fluorescent peptide to decellularized tissue versus decellularized tissue alone. In addition, the studies conducted on human tissue utilized a smaller sample size due to shortage of human tissue availability. The smaller sample size may have contributed to the lack of statistical significance, as often a small sample size results in more conservative estimates of significance. Ultimately, our study shows the reliability of our methods to covalently attach an RGD peptide to decellularized tissue and enhance HUVEC adhesion to the surface of RGD functionalized decellularized tissue. The comparability of our work to a clinically significant model of human tissue furthers the promise of this method of EC repopulation onto decellularized scaffolds. This study also

110

highlights the benefit of doing proof of concept studies in animal models prior to testing on human tissue. By optimizing conditions in an animal model and applying these *in-vitro* methods to human tissue which is in short supply for research purposes, more human tissues will be available for research use. Thus most *in-vitro* tissue engineering studies can be tested on more abundant tissues such as ovine or porcine tissues with confidence that the results will transfer to human tissues. This may prevent disastrous clinical studies such as the Synergraft valve (28).

3.2   FUTURE DIRECTIONS:

Our studies do not show functionality of ECs seeded onto decellularized scaffolds. This was primarily due to the use of a commercial cell line. Future studies should utilize a cell source of EC progenitors that are isolated fresh from recipients and characterized. Functionality of these autologous cells once seeded onto decellularized RGD scaffolds will be of utmost importance. Endothelial nitric oxide synthase is a well known measure of EC function *in-vitro*. HUVEC do not express eNOS, however, valvular ECs do. Thus, the logical next step would be to isolate and characterize an appropriate cell source such as HUCBSCs and evaluate these for eNOS secretion and native valvular endothelial cell structure and function. In addition, platelet adhesion tests would be necessary in order to show attenuation of thrombogenicity of recellularied decellularized scaffolds.

The RGD binding process has the potential to modify the collagen fibres of the decellularized allograft and could thereby affect the mechanical properties of the graft. The repopulating endothelial cells too may secrete factors that could alter the collagen structure. Thus, appropriate mechanical strength studies should be conducted on whole decellularized RGD modified tissue patches recellularized with endothelial cells.

Following an *in-vitro* 3 day HUVEC seeding protocol, *in-vitro* cell retention should be evaluated using a bioreactor. A bioreactor which mimics physiological pH, flow rate, pressure, O2 and CO2 gradients and shear stress will be able to accurately evaluate neoendothelium cell retention on the surfaces of RGD modified decellularized tissue.

In-vitro work in tissue engineering of decellularized scaffolds should also assess a method for repopulation of ECM with interstitial cells. An intrinsic component to valve and tissue function, ICs will be necessary for remodeling of the collagen structure and repair of damaged tissue (29). Studies have looked into the repopulation of decellularized scaffolds using MSCs injected directly into the ECM (30). This may be a promising approach to decellularized tissue repopulated with ECs along the luminal surface.

Finally, a large animal model will be necessary to show improved outcomes prior to the translation to the clinic. Sheep models are generally the accepted large animal model for transplantation and tissue valve studies as mandated by the FDA due to their increased rates of calcification. An *in-vivo* large animal model would need to include a measure of the allogenicity of

112

animals donating and receiving grafts (31), a method for isolation and

characterization of autologous sheep cells for the repopulation of decellularized

tissues, *in-vitro* seeding for 3 days following our results, implantation, ECG at

regular time intervals to assess cardiac function, serum antibody level

measurements and platelet activation and finally, a measure of the confluency of

the reseeded decellularized patches upon explantation.

3.3   OVERALL GOAL

As previously stated, an ideal valve replacement would be be non-

immunogenic, non-thrombogenic and have the capacity to grow and repair itself

in-vivo. This research has made significant headway into the repopulation of

decellularized allograft scaffolds for use in congenital cardiac surgery, however,

there is still more research necessary before the ideal valve replacement can be

realized. The ultimate goal of cardiac valve tissue engineering is to one day

develop a multi-tissue structure composed of endothelial and interstitial cells

which is capable of remodeling and repairing the ECM the same as a native valve.

Additional advances in stem cell and ECM understanding will further the search

for the ideal cardiac valve replacement, but the exciting possibility comes one

step closer to reality every day.

3.4 CONCLUSIONS

The experiments in this thesis have made significant advancements in the field of tissue engineering of decellularized allograft tissue used in congenital cardiac surgery. Significant findings include:

   I. Increasing the hypotonic and hypertonic and tris-washout steps of our published decellularization protocol from 48 hours to 72 hours further removes cellular debris that is not completely removed in ovine and human tissue,

  II. A method to covalently bind a fluorescently labeled RGD peptide to decellularized tissue

 III. The addition of an enzymatically reacted maleimide group to bind the FITC labeled RGD peptide to decellularized tissue is not necessary, decellularized collagen will bind the RGD-FITC peptide in the presence of water or MES buffer alone

 IV. An optimal concentration of 50μM of the RGD-FITC peptide will covalently bind almost 100% of $1x10^6$ HUVEC cells

  V. We have shown quantitatively, evidence of increased HUVEC binding to RGD-modified decellularized tissue than decellularized tissue alone

 VI. We have determined the optimal HUVEC concentration for re-endothelialization of decellularized tissue to be 1×10^6 cells/$30mm^2$

VII. At 36 hours, RGD peptide appears to enhance HUVEC migration to the endothelial surface compared to decellularized surface alone

VIII. At 72 hours after cell incubation, HUVEC cells appear to adhere to the luminal surface and lay flat

 IX. At 8 days after cell incubation cell adhesion does not appear to reach confluence indicating that 3 days is likely the optimal incubation time for *in-vitro* static recellularization of decellularized tissue

  X. Determination of the ovine model of recellularization of decellularized tissue as a reproducible and reliable optimization of *in-vitro* tissue engineering studies using human decellularized tissue

 XI. Overnight chymotrypsin digestion of the 18 AA peptide results in successful cleavage of the potentially immunogenic FITC fragment while retaining the RGD sequence of interest for our experiments

3.5 REFERENCES

1. Hogan PG, O'Brien MF. Improving the allograft valve: Does the immune response matter? J Thorac Cardiovasc Surg. 2003 Nov [cited 3/31/2008];126(5):1251-3.

2. Baskett RJ, Ross DB, Nanton MA, Murphy DA. Factors in the early failure of cryopreserved homograft pulmonary valves in children: Preserved immunogenicity? J Thorac Cardiovasc Surg. 1996 Nov;112(5):1170,8; discussion 1178-9.

3. Dignan R, O'Brien M, Hogan P, Thornton A, Fowler K, Byrne D, et al. Aortic valve allograft structural deterioration is associated with a subset of antibodies to human leukocyte antigens. J Heart Valve Dis. 2003 May;12(3):382,90; discussion 390-1.

4. Rose EA, Pepino P, Barr ML, Smith CR, Ratner AJ, Ho E, et al. Relation of HLA antibodies and graft atherosclerosis in human cardiac allograft recipients. J Heart Lung Transplant. 1992 May-Jun;11(3 Pt 2):S120-3.

5. Jegatheeswaran A, Butany J. Pathology of infectious and inflammatory diseases in prosthetic heart valves. Cardiovasc Pathol. 2006 Sep-Oct;15(5):252-5

6. Bruck SD. Possible causes for the calcification of glutaraldehyde-treated tissue heart valves and blood contacting elastomers during prolonged use in medical devices: A physico-chemical view. Biomaterials. 1981 Jan;2(1):14-8.

7. O'Brien MF, Goldstein S, Walsh S, Black KS, Elkins R, Clarke D. The SynerGraft valve: A new acellular (nonglutaraldehyde-fixed) tissue heart valve for autologous recellularization first experimental studies before clinical implantation. Semin Thorac Cardiovasc Surg. 1999 Oct;11(4 Suppl 1):194-200.

8. Cowan PJ, d'Apice AJ. Complement activation and coagulation in xenotransplantation. Immunol Cell Biol. 2009 Mar-Apr;87(3):203-8.

9. Boneva RS, Folks TM. Xenotransplantation and risks of zoonotic infections. Ann Med. 2004;36(7):504-17.

10. Gall KL, Smith SE, Willmette CA, O'Brien MF. Allograft heart valve viability and valve-processing variables. Ann Thorac Surg. 1998 Apr;65(4):1032-8.

11. Shaddy RE, Hawkins JA. Immunology and failure of valved allografts in children. Ann Thorac Surg. 2002 Oct;74(4):1271-5.

12. Lehr EJ, Hermary S, McKay RT, Webb DN, Abazari A, McGann LE, et al. NMR assessment of me(2)SO in decellularized cryopreserved aortic valve conduits. J Surg Res. 2007 Jul;141(1):60-7.

13. Mendelson K, Schoen FJ. Heart valve tissue engineering: Concepts, approaches, progress, and challenges. Ann Biomed Eng. 2006 Dec;34(12):1799-819.

14. Lichtenberg A, Tudorache I, Cebotari S, Suprunov M, Tudorache G, Goerler H, et al. Preclinical testing of tissue-engineered heart valves re-endothelialized under simulated physiological conditions. Circulation. 2006 Jul 4 [cited 3/31/2008];114(1 Suppl):I559-65.

15. Seebacher G, Grasl C, Stoiber M, Rieder E, Kasimir MT, Dunkler D, et al. Biomechanical properties of decellularized porcine pulmonary valve conduits. Artif Organs. 2008 Jan;32(1):28-35.

16. Takagi K, Fukunaga S, Nishi A, Shojima T, Yoshikawa K, Hori H, et al. In vivo recellularization of plain decellularized xenografts with specific cell characterization in the systemic circulation: Histological and immunohistochemical study. Artif Organs. 2006 Apr;30(4):233-41.

17. Kaushal S, Amiel GE, Guleserian KJ, Shapira OM, Perry T, Sutherland FW, et al. Functional small-diameter neovessels created using endothelial progenitor cells expanded ex vivo. Nat Med. 2001 Sep;7(9):1035-40.

18. Meinhart JG, Schense JC, Schima H, Gorlitzer M, Hubbell JA, Deutsch M, et al. Enhanced endothelial cell retention on shear-stressed synthetic vascular grafts precoated with RGD-cross-linked fibrin. Tissue Eng. 2005 May-Jun;11(5-6):887-95.

19. Stile RA, Shull KR, Healy KE. Axisymmetric adhesion test to examine the interfacial interactions between biologically-modified networks and models of the extracellular matrix. Langmuir. 2003;19(5):1853-60.

20. Reulen SW, Brusselaars WW, Langereis S, Mulder WJ, Breurken M, Merkx M. Protein-liposome conjugates using cysteine-lipids and native chemical ligation. Bioconjug Chem. 2007 Mar-Apr;18(2):590-6

21. Engelmayr GC,Jr, Sales VL, Mayer JE,Jr, Sacks MS. Cyclic flexure and laminar flow synergistically accelerate mesenchymal stem cell-mediated engineered tissue formation: Implications for engineered heart valve tissues. Biomaterials. 2006 Dec;27(36):6083-95.

22. Pierschbacher MD, Ruoslahti E. Cell attachment activity of fibronectin can be duplicated by small synthetic fragments of the molecule. Nature. 1984 May 3-9;309(5963):30-3.

23. Mirsadraee S, Wilcox HE, Watterson KG, Kearney JN, Hunt J, Fisher J, et al. Biocompatibility of acellular human pericardium. J Surg Res. 2007 Dec;143(2):407-14.

24. Nagai T. A second cell recognition site of fibronectin. Seikagaku. 1991 Jul;63(7):507-12.

25. Iop L, Renier V, Naso F, Piccoli M, Bonetti A, Gandaglia A, et al. The influence of heart valve leaflet matrix characteristics on the interaction between human mesenchymal stem cells and decellularized scaffolds. Biomaterials. 2009 May 27.

26. Sechler JL, Takada Y, Schwarzbauer JE. Altered rate of fibronectin matrix assembly by deletion of the first type III repeats. J Cell Biol. 1996 Jul;134(2):573-83.

27. Hynes, R.O., 1990. Fibronectins. Springer-Verlag Inc., New York.

28. Simon P, Kasimir MT, Seebacher G, Weigel G, Ullrich R, Salzer-Muhar U, et al. Early failure of the tissue engineered porcine heart valve SYNERGRAFT in pediatric patients. Eur J Cardiothorac Surg. 2003 Jun [cited 4/1/2008];23(6):1002,6; discussion 1006.

29. Hinton RB,Jr, Lincoln J, Deutsch GH, Osinska H, Manning PB, Benson DW, et al. Extracellular matrix remodeling and organization in developing and diseased aortic valves. Circ Res. 2006 Jun 9 [cited 3/31/2008];98(11):1431-8.

30. Vincentelli A, Wautot F, Juthier F, Fouquet O, Corseaux D, Marechaux S, et al. In vivo autologous recellularization of a tissue-engineered heart valve: Are bone marrow mesenchymal stem cells the best candidates? J Thorac Cardiovasc Surg. 2007 Aug;134(2):424-32

31. Lehr EJ, Rayat GR, Desai LS, Coe JY, Korbutt GS, Ross DB. Inbred or outbred? an evaluation of the functional allogenicity of farm sheep used in cardiac valve studies. J Thorac Cardiovasc Surg. 2006 Nov;132(5):1156-61.